



ENVIRONMENTAL SCIENCE

ISSN 0250-3301 CODEN HCKHDV HUANJING KEXUE

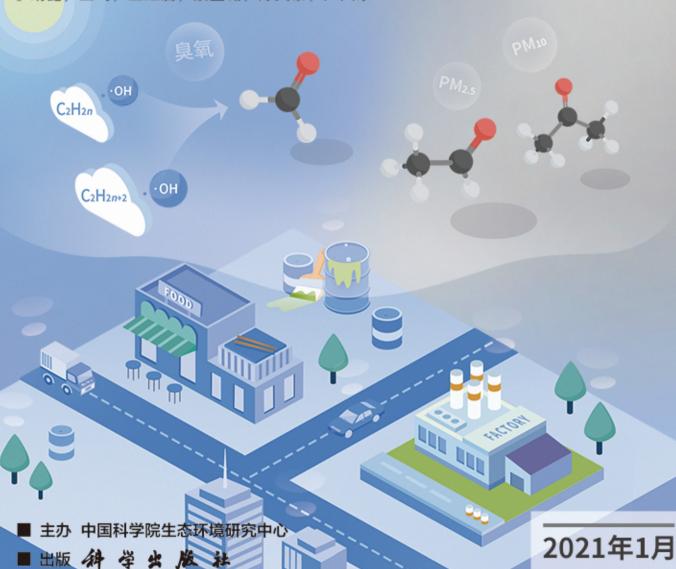
第42卷

Vol.42

第1期

No.1

基于PMF和源示踪物比例法的大气羰基化合物来源解析:以南京市观测为例 胡崑,王鸣,王红丽,景盛翱,陈文泰,卢兴东



ENVIRONMENTAL SCIENCE

第42卷 第1期 2021年1月15日

目 次

2019 年国庆节前后北京气态氨和气溶胶铵盐浓度的同步观测 ·····	
··················· 顾梦娜,潘月鹏,宋琳琳,李萍,田世丽,武岳洋,杨婷婷,李浩洋,石生伟,吐莉尼沙,吕雪梅,孙倩,方运霆(1)	١
世工工上机探穴和粉估增担工油。发表运流出租公坛。	,
基于无人机探空和数值模拟天津一次重污染过程分析 ····································	,
中原项甲杆典型项甲代令学人飞上M _{2.5} 行架行征及馈源	,
沈阳市冬季大气 PM _{2.5} 中水溶性离子污染特征及来源解析)
基于 PMF 和源示踪物比例法的大气羰基化合物来源解析:以南京市观测为例 胡崑,王鸣,王红丽,景盛翱,陈文泰,卢兴东(45)	
2019 年天津市挥发性有机物污染特征及来源····································)
柳州市春季大气挥发性有机物污染特征及源解析 刘齐,卢星林,曾鹏,于奭(65))
天津市郊夏季的臭氧变化特征及其前体物 VOCs 的来源解析 罗瑞雪,刘保双,梁丹妮,毕晓辉,张裕芬,冯银厂(75))
2017 年春夏期间南京地区臭氧污染输送影响及潜在源区	
)
2006~2019年珠三角地区臭氧污染趋势 赵伟,高博,卢清,钟志强,梁小明,刘明,马社霞,孙家仁,陈来国,范绍佳(97))
大型石化企业邻近区域大气沉降中多环芳烃赋存特征及源解析 李大雁,齐晓宝,吴健,黄沈发,王敏,沙晨燕,沈城(106))
叶片大气颗粒物滞纳能力评估方法的定量对比)
东江流域敌敌畏的排放量估算及归趋模拟 张冰、张芊芊、应光国(127))
松花江哈尔滨段及阿什河抗生素的分布规律与生态风险评估 杨尚乐,王旭明,王伟华,胡雪莹,高立伟,孙兴滨(136))
东北小兴凯湖沉积物 POPs 污染特征及生态风险评价·························李慧,李捷,宋鹏,程云轩,焦立新,杨亚铮(147))
河南省地表水源中 PPCPs 分布及生态风险评价)
无锡-常州地下水中内分泌干扰物的赋存特征和健康风险评价 王淑婷,饶竹,郭峰,刘成海,战楠,王娅南,彭洁,杨鸿波(166)	١
清江流域地表水重金属季节性分布特征及健康风险评价	١
会仙岩溶湿地丰平枯时期地下水金属元素污染与健康风险 李军,赵一,邹胜章,蓝芙宁,樊连杰,谢浩,秦月,朱丹尼(184)	١
二岐床区城镇化影响下河流 DOM 光谱蛙征季节变化	١
三峡库区城镇化影响下河流 DOM 光谱特征季节变化 ····································	١
基于宏基因组学探讨东平湖水库的菌群结构、耐药基因谱及其公共健康风险 张红娜、崔娜、申红妙(211)	'
委」 公奉囚组子环门尔干·彻尔岸的国研扫构、侧约奉囚眉及兵公共健康风险 ····································	
刀云望小件裸尖字相便管的细图性肝脏切机制	,
丹江口库区浮游真菌组成与功能及其影响因素 ························· 郑保海,王晓宇,李英军,陈彦,李百炼,李玉英,陈兆进(234) 太湖出流河道藻颗粒变化及其水质效应 ····································)
人例出流刊担梁积杜受化及共小贝双州 "" 却于凡,计冯,陈旭滨,却廷平,信旭,木广伟,木罗则(242))
石盘丘小流域不同土地利用方式下土壤氮磷流失形态及通量 ····································)
即期十早大致刈生物滞留系统际炎性能的影响)
浒苔生物炭对雨水径流中氨氮的吸附特性及吸附机制 陈友媛,李培强,李闲驰,孙萍,赵新月,李洁,李晋,辛至然(274))
填料对潮汐流人工湿地中 CANON 作用强化的影响)
FeMnN1-LDHs 对水中As(Ⅲ)的吸附性能与机制)
硝酸钙添加和锆改性膨润土覆盖联用控制底泥中磷释放的效果及机制 张宏华,林建伟,詹艳慧,俞阳,张志斌(305))
某市污水厂抗生素和抗生素抗性基因的分布特征)
不同污泥在微波预处理-厌氧消化过程中抗性基因分布及菌群结构演替 李慧莉,武彩云,唐安平,佟娟,魏源送(323))
天然富硒土地划定的富硒阈值 王惠艳,曾道明,郭志娟,成晓梦,彭敏,孙跃(333))
融合自然-人为因子改进回归克里格对土壤镉空间分布预测。高中原,肖荣波,王鹏,邓一荣,戴伟杰,刘楚藩(343))
南方典型水稻土镉(Cd)累积规律模拟······ 戴雅婷, 傅开道, 杨阳, 王美娥, 陈卫平(353))
闽西南土壤-水稻系统重金属生物可给性及健康风险 林承奇,蔡宇豪,胡恭任,于瑞莲,郝春莉,黄华斌(359))
干湿交替灌溉制度下纳米修复材料对杂交籼稻籽粒 Cd 累积及产量的影响 ····································	
杨茹,陈馨睿,张颖,崔俊义,武立权,马友华,廖江,何海兵(368))
三元复合调理剂对土壤镉砷赋存形态和糙米镉砷累积的调控效应 蒋毅,刘雅,辜娇峰,杨世童,曾雄,王轩宁,周航,廖柏寒(378)	
风化煤组配改良剂结合水分管理对水稻根际土壤与稻米甲基汞含量的影响 郑顺安,吴泽嬴,杜兆林,倪润祥,姚启星(386))
不同施肥措施对水稻土壤微生物镉抗性的影响 郑开凯,马志远,孙波,梁玉婷(394)	
氮添加影响下新疆天山雪岭云杉林土壤酶活性及其与环境因子的相关性 张涵,贡璐,刘旭,邵康,李昕竹,李蕊希(403)	
黄土丘陵区撂荒农田土壤酶活性及酶化学计量变化特征 钟泽坤,杨改河,任成杰,韩新辉(411)	
生物炭对土壤酶活和细菌群落的影响及其作用机制 冯慧琳、徐辰生、何欢辉、曾强、陈楠、李小龙、任天宝、姬小明、刘国顺(422))
植被恢复对刺萼龙葵根际土壤细菌群落结构与功能的影响 张瑞海,宋振,付卫东,郓玲玲,高金会,王然,王忠辉,张国良(433)	
黄壤稻田土壤微生物量碳氮及水稻品质对生物炭配施氮肥的响应 史登林,王小利,刘安凯,侯再芬,梁国太(443)	
等碳量添加秸秆和生物炭对土壤呼吸及微生物生物量碳氮的影响 何甜甜,王静,符云鹏,符新妍,刘天,李亚坤,李建华(450))
秸秆与氮肥配比对农田土壤内外源碳释放的影响 孙昭安,张轩,胡正江,王开永,陈清,孟凡乔(459))
生物炭与化肥混合对氨挥发和磷固定的影响)
氮肥减投条件下膜材料使用对稻田氨挥发排放的影响)
微塑料对斑马鱼胚胎孵化影响及其在幼鱼肠道中的积累)
无人机热红外支持下的城市微尺度热环境模拟 阳少奇, 冯莉, 田慧慧, 刘艳霞(492))
基于人居尺度的中国城市热岛强度时空变化及其驱动因子解析)
《环境科学》征订启事(8) 《环境科学》征稿简则(220) 信息(233,352,421)	



FeMnNi-LDHs 对水中As(Ⅲ)的吸附性能与机制

廖玉梅, 余杰, 魏世强, 蒋珍茂*

(西南大学资源环境学院,重庆市农业资源与环境研究重点实验室,重庆 400715)

摘要:稳定和高效地去除地下水中的As(\blacksquare) 仍然是一个具有挑战的全球性问题.本研究以 Fe、Mn 和 Ni 这 3 种元素作为层板阳离子,采用共沉淀法制备出三金属层状双氢氧化物 FeMnNi-LDHs,利用 XRD、TEM、FT-IR 和 XPS 等技术对其结构进行表征,并探讨其对水中As(\blacksquare) 的吸附去除能力与机制. 结果表明,FeMnNi-LDHs 具有层状双氢氧化物的典型特征峰,峰型尖锐,结晶度高,TEM 图像也显示有明显的层状结构. 其对 As(\blacksquare) 的吸附动力学符合准二级动力学模型,等温吸附曲线符合Freundlich 等温方程,45℃时最大吸附量为 240. 86 mg·g⁻¹,明显高于其他层状双氢氧化物. 在 pH 为 2 ~ 9 范围内,FeMnNi-LDHs 对As(\blacksquare) 均有较好的吸附效果. 水中共存 PO_4^{3-} 和 CO_3^{2-} 离子对As(\blacksquare))存在竞争吸附,而 NO_3^{-} 、 Cd^{2+} 和 Pb^{2+} 影响较小. 其去除吸附机制主要为氧化、离子交换和配位络合,其中 Mn 在As(\blacksquare) 的氧化过程中有重要贡献. 制备出的 FeMnNi-LDHs 对水中As(\blacksquare) 的吸附去除和毒性控制具有良好的应用潜力.

关键词:层状双氢氧化物(LDHs); 砷(As); 氧化; 吸附去除; 毒性控制

中图分类号: X131.2; X52 文献标识码: A 文章编号: 0250-3301(2021)01-0293-12 DOI: 10. 13227/j. hjkx. 202005012

Adsorption Effect and Mechanism of Aqueous Arsenic on FeMnNi-LDHs

LIAO Yu-mei, YU Jie, WEI Shi-qiang, JIANG Zhen-mao*

(Chongqing Key Laboratory of Agricultural Resources and Environment Research, College of Resources and Environment, Southwest University, Chongqing 400715, China)

Abstract: Removing As(\blacksquare) from water steadily and efficiently is still a challenging global issue. In this study, novel FeMnNi-LDHs were prepared by a co-precipitation method using Fe, Mn, and Ni as lamellar cations, and the structure were characterized by XRD, TEM, FT-IR, and XPS techniques, and the adsorption performance and mechanism of As(\blacksquare) was explored. The results showed that FeMnNi-LDHs have typical characteristic peaks of layered double hydroxides, with sharp peaks and high crystallinity. The TEM images also show obvious layered structures. The adsorption kinetics of As(\blacksquare) on FeMnNi-LDHs agree with the quasi second-order kinetic model, and the isotherm adsorption curve agrees with the Freundlich isotherm equation. The maximum adsorption capacity at 45 °C was 240. 86 mg·g⁻¹, which is significantly higher than other similar layered double hydroxides. Acidity had little effect on the adsorption performance of As(\blacksquare), and it had a good adsorption effect in the range of pH 2-9. The coexistence of PO₄³⁻ and CO₃²⁻ ions in water showed adverse effects on the As(\blacksquare) adsorption capacity, and NO₃⁻, Cd²⁺, and Pb²⁺ had less influence. The adsorption mechanism of FeMnNi-LDHs for As(\blacksquare) includes ion exchange, oxidation, and coordination complexation, in which Mn plays a major role in the oxidation process of As(\blacksquare). The prepared FeMnNi-LDHs exhibited good application potential in the adsorption of As(\blacksquare) from water and toxicity control.

Key words: layered double hydroxides (LDHs); arsenic (As); oxidation; adsorption removal; toxicity control

神(As)是一种普遍存在于自然界中,具有毒性的类金属元素,已被国际癌症研究机构(IARC)归为A类致癌物质^[1,2]. 长期接触和摄入砷污染的水会对人体健康造成严重的影响,如皮肤损伤、坏疽、肾衰竭和癌症等^[3]. 在自然环境中,As 主要以无机形态:砷酸盐As(V)和亚砷酸盐As(Ⅲ)形式存在,As(Ⅲ)比As(V)的毒性高约100倍,并且大量存在于地下含水层等厌氧条件下,难以被含水层固相吸附^[4]. 相较于As(V),As(Ⅲ)被认为毒性更高,更易溶解,更易迁移,更难以去除. 目前,水体除砷的方法主要有混凝沉淀法^[5]、离子交换法^[6]、膜分离法^[7]、生物法^[8]和吸附法^[9]等. 其中吸附法因成本低、处理效果优良、操作简单和绿色环保等优点而受到关注^[10].

层状双氢氧化物 (layered double hydroxides,

LDHs) 是一类阴离子黏土,具有与水镁石 [Mg (OH)₂]相似的层状结构,因其良好的热稳定性、记忆效应、亲水性和较高的阴离子交换能力已被广泛用于废水治理^[11]. LDHs 作为具有较好潜力的水中砷去除剂,受到不少研究者的关注. Maziarz 等^[12]将MgAl-LDHs 浸渍铁氧化物颗粒制备出磁性层状双氢氧化物,对As(V)的吸附表现出优异的效果,最大吸附量可达 90. 60 mg·g⁻¹. Lee 等^[13]将 MgAl-LDHs 在 400℃煅烧后,发现其对As(V)的吸附效果有了大幅地提升,最大吸附量由 19. 70 mg·g⁻¹增加到了

收稿日期: 2020-05-03;修订日期: 2020-06-30

基金项目: 国家重点研发计划项目(2018YFD0800600); 中央高校基本 # 4 # 4 # 5 # (VPW2010P045)

本业务费专项(XDJK2018B045)

作者简介: 廖玉梅(1995~),女,硕士研究生,主要研究方向为环境 功能材料对水体和土壤修复,E-mail; yumei951220@163.

* 通信作者,E-mail:windring@swu.edu.cn

102. 90 mg·g⁻¹. 最近, Lee 等^[14]将 CoAl-LDHs 负载 在勃姆石表面吸附As(V),发现大部分的As(V)可以通过离子交换和形成双齿-双核内球络合物而被吸附. 已有的研究大多着重于As(V)去除,而有关吸附As(III)的报道仍然较少,这主要是因为As(III)在水中通常以电中性的 H_3 AsO₃ 形态存在,对吸附剂表面亲和力较低,较As(V)更难以去除^[15]. 为增加其亲和力,通常需要将As(III)进行氧化预处理转化为As(V). 因此制备出一种有氧化能力的层状双氢氧化物,可望实现对As(III)的同步氧化和高效吸附去除.

有研究表明,锰(氢)氧化物可在较宽的 pH 范 围内将As(Ⅲ)氧化为As(V),常作为砷的氧化剂, 铁(氢)氧化物具有较高的亲和力可提高As(Ⅲ)的 吸附能力[16]. 然而由于铁锰自身的氧化性,可导致 晶体产生紊乱和层状结构坍塌,难以制备出完整层 状结构的铁锰类 LDHs. Zhou 等[17] 创造性地在共沉 淀法体系中引入 Mg2+,成功制备出了具有良好层状 结构的三金属层状双氢氧化物: FeMnMg-LDHs, 但 该材料在 pH 为 2~6 时 Mg²⁺溶出率高达 10%,且吸 附 Pb2+后材料层状结构坍塌,稳定性还有待提高. 本研究尝试选用与 Mg 同族元素 Ni 作为离子稳定 剂,Ni属于稀土元素,因其良好的导电性,是经典的 电容材料,近年来也被广泛运用于水污染处理 中[18~20]. Ni 原子半径与 Fe、Mn 原子半径更相近 预期可以与 Fe 和 Mn 紧密结合,提高材料稳定性, 并且 Ni 原子容易发生价态的变化, 也可能实现 As(Ⅲ)的氧化. 采用共沉淀法制备出的 FeMnNi-LDHs 被证实具有典型 LDHs 层状结构,稳定性得以 进一步提升. 通过改变反应时间、初始浓度、pH 和竞 争离子研究了 FeMnNi-LDHs 对As(Ⅲ) 的吸附性能 和影响因素,采用 XRD、TEM、FT-IR 和 XPS 对吸附 As(Ⅲ)前后的 FeMnNi-LDHs 进行表征分析,探究了 所制备的 FeMnNi-LDHs 对As(Ⅲ)的去除机制.

1 材料与方法

1.1 实验试剂

实验试剂:NiCl₂·6H₂O(AR,成都市科隆化学品有限公司),FeCl₃·6H₂O(AR,成都市科龙化工试剂厂),MnCl₂·4H₂O(AR,成都市科龙化工试剂厂),NaOH(AR,成都市科龙化工试剂厂),KBH₄(AR,国药集团化学试剂有限公司),(NH₂)₂CS(AR,国药集团化学试剂有限公司),C₆H₈O₆(AR,国药集团化学试剂有限公司),NaAsO₂(GR,国药集团化学试剂有限公司).其它试剂均为分析纯.本实验中所用溶液均由去离子水和超纯水配制.

1.2 材料的制备方法

FeMnNi-LDHs 的制备采用共沉淀法^[21]. 准确称取 11.885 g NiCl₂·6H₂O(0.05 mol)、6.825 g FeCl₃·6H₂O(0.025 mol)和 4.947 g MnCl₂·4H₂O(0.025 mol)溶于50 mL 去离子水中,搅拌均匀配制混合金属离子溶液.向500 mL 的三颈烧瓶中加入 100 mL 去离子水,用 2 mol·L⁻¹ NaOH 溶液调节去离子水pH 为 10,通人氮气持续 10 min. 将混合金属离子溶液逐滴加入三颈烧瓶内,并用机械搅拌,同时滴加碱液保持溶液 pH 为 10.滴加完成后,持续通入氮气,机械搅拌 2 h. 搅拌完成后用塑料膜封闭三颈烧瓶瓶口,放入水浴锅,60℃恒温水浴 15 h. 水浴后的固体产物使用无氧水冲洗至上清液呈中性,离心,冷冻干燥 48 h. 干燥后的产物用玛瑙研钵磨碎过 100 目筛,妥善密封保存于干燥箱中,备用.

1.3 材料的结构表征

FeMnNi-LDHs 成分组成使用德国布鲁克公司 D8 ADVANCE 型 X 粉末衍射仪分析,测试条件为: X 射线源为 Cu 靶 K α (λ = 0.154 18 nm),电压 40 kV,电流 40 mA. 材料形貌像采用美国 FEI 公司 Tecnai G2 F20 场发射透射电子显微镜扫描,加速电压为 200 kV. 材料鉴定分析采用美国尼高力公司 Nicolet IS10 尼高力红外光谱仪. 材料元素价态分析采用美国赛默飞公司 Escalab 250Xi 型 X 射线光电子能谱仪.

1.4 吸附等温实验

准确称取 0.050 g 材料于一系列 100 mL 锥形瓶中,分别加入 50 mL 质量浓度为 5、10、20、50、100、300、600、1000、1500 和 2000 mg·L⁻¹ As(III)溶液 (每组实验重复 3 次),使用 0.1 mol·L⁻¹ NaOH或 0.1 mol·L⁻¹ HCl 调节溶液 pH 为 5.5 ± 0.1 ,分别于 25、35 和 45 $^{\circ}$ 恒温振荡器振荡 24 h,转速为 180 r·min⁻¹,20.45 20.45

1.5 吸附动力学实验

准确称取 0.050 g 材料于1000 mL 的锥形瓶中,分别加入 1000 mL 质量浓度为 10、20 和 50 mg·L⁻¹ As(\blacksquare) 溶液,使用 0.1 mol·L⁻¹ NaOH 或 0.1 mol·L⁻¹ HCl 调节溶液 pH 为 5.5 ± 0.1 ,将锥形瓶分别置于 25 $^{\circ}$ 恒温振荡器振荡,转速为 180 r·min⁻¹,分别于 10、30、60、240、480、720 和 1440 min 取 10 mL 样品,使用 0.45 μ m 滤膜过滤,稀释,溶液中As(\blacksquare)的质量浓度采用 ICP-OES 测定.

吸附平衡后溶液中As(Ⅲ)的吸附量通过公式(1)计算:

$$q_e = V(c_0 - c_e)/m \tag{1}$$

式中, q_e 为平衡吸附量($mg \cdot g^{-1}$), c_0 为吸附前 $As(\coprod)$ 质量浓度($mg \cdot L^{-1}$), c_e 为吸附平衡时 $As(\coprod)$ 质量浓度($mg \cdot L^{-1}$),V 为溶液体积(mL),m 为材料投加量(g).

1.6 pH 对材料吸附As(Ⅲ)的影响

准确称取 0.050 g 材料于一系列 100 mL 锥形瓶中,分别加入 50 mL 质量浓度为 20 mg·L⁻¹的 As(III)溶液.用 0.1 mol·L⁻¹ NaOH 或 0.1 mol·L⁻¹ HCl 调节溶液 pH 分别为: 2.3.4.5.6.7.8.9.10.11 和 12(每组实验重复 3 次).于 <math>25% 恒温振荡器振荡 24 h,转速为 180 r·min⁻¹, 20.45 2

1.7 竞争离子对材料吸附As(Ⅲ)的影响

准确称取 0.050 g 材料于一系列 100 mL 锥形瓶中,分别加入 50 mL 质量浓度为 50 mg·L⁻¹ $As(\mathbb{II})$ 和 PO_4^{3-} 、 CO_3^{2-} 、 NO_3^- 、 Cd^{2+} 和 Pb^{2+} (0、10、20、50、80 和 <math>100 mg·L⁻¹)的混合溶液(其中 PO_4^{3-} 、 CO_3^{2-} 、 NO_3^- 、 Cd^{2+} 和 Pb^{2+} 溶液分别采用 Na_3PO_4 、 Na_2CO_3 、 $NaNO_3$ 、 $CdCl_2$ 和 $PbCl_2$ 配制,每组实验重复 3 次),使用 0.1 mol·L⁻¹ NaOH 或 0.1 mol·L⁻¹ HCl 调节溶液 pH 为 5.5 ± 0.1 ,于 25% 恒温振荡器振荡 24 h,转速为 180 r·min⁻¹,经 0.45 μm 滤膜抽滤,稀释,溶液中 $As(\mathbb{II})$ 的质量浓度采用 ICP-OES测定.

1.8 数据分析

本实验数据采用 Excel 2012 与 Origin 8.5 进行处理与作图.

2 结果与讨论

2.1 材料表征分析

FeMnNi-LDHs 材料的 XRD 分析结果如图 1 所示,材料在 2θ 为 11.10° 、 22.30° 、 33.52° 、 39.22° 、46. 80° 、59. 74° 和 61.14° 处都有尖锐的特征峰,这些峰分别对应(003)、(006)、(009)、(015)、(018)、(110)和(113)晶面,与层状双氢氧化物特征衍射峰(PDF No.51-1525)相符,表明引入 Ni 原子成功地制备出了三金属层状双氢氧化物 FeMnNi-LDHs. 2θ 为 11.10° 、 22.30° 和 33.52° 处的特征峰呈现良好的倍数关系,且在 60° ~ 63° 之间的(110)和(113)峰型尖锐容易辨认,说明合成的 FeMnNi-LDHs 结晶度高,晶体结构完整,晶相也比较单一 $[^{22}]$.可以根据公式 $a=2d(110)^{[23]}$ 、 $c=d(003)+2d(006)+3d(009)^{[14]}$ 计算得到 FeMnNi-LDHs 的晶格常数; a=

0. 309 5 nm、c = 2.3964 nm,其中 a 表示金属离子之比 M^{2+}/M^{3+} ,d 表示晶面的层间距,c 表示层状双氢氧化物的层间距。a 与实际制备时摩尔比 $Fe^{3+}/(Mn^{2+}+Ni^{2+})=0.3333$ 相差较小,说明制备过程清洁稳定;a、c 值与典型的层状双氢氧化物相近^[24],进一步说明制备出的材料是层状双氢氧化物.

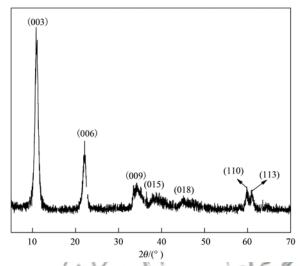


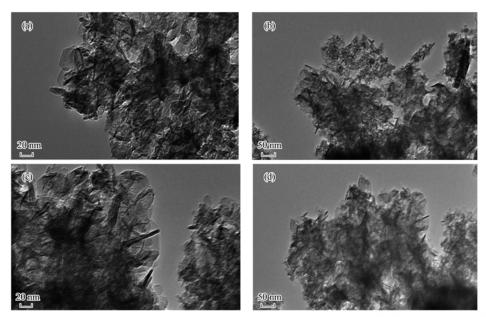
图 1 FeMnNi-LDHs 的 XRD 图谱 Fig. 1 XRD pattern of FeMnNi-LDHs

FeMnNi-LDHs 吸附As(III)前后的形貌像如图 2 所示. 图 2(a)和 2(b)为吸附前的 FeMnNi-LDHs 形貌,能清晰地观察到片层结构,部分晶体边缘呈典型的六边形结构,但片层紧密排列,相互重叠,团聚现象较为明显^[20]. 吸附后的 FeMnNi-LDHs 仍然能观察到良好的完整片层结构[如图 2(c)和 2(d)],吸附前后材料结构变化小,相比于周宏光^[25]制备的FeMnMg-LDHs 吸附 Pb²⁺后材料由完整的片层结构变成了破碎状态,本研究制备的 FeMnNi-LDHs 具有更好的稳定性能,可以实现材料的重复使用.

2.2 等温吸附实验

FeMnNi-LDHs 在 25、35 和 45℃ 对As(\blacksquare) 的等温吸附曲线如图 3 所示. 当溶液中As(\blacksquare) 初始质量浓度为 0 ~ 2 000 mg·L⁻¹时,材料对As(\blacksquare) 的吸附量随初始质量浓度增加而快速增加.

分别使用 Langmuir 和 Freundlich 吸附模型对等温吸附曲线进行拟合,拟合的相关参数如表 1 所示. Langmuir 和 Freundlich 对等温吸附曲线均有较好的拟合结果,但相较于 Langmuir 等温吸附模型, Freundlich 等温吸附模型能更好地描述 FeMnNi-LDHs 吸附 As(\blacksquare) 过程,说明 FeMnNi-LDHs 对As(\blacksquare)的吸附是多分子层吸附过程,其它研究也有相似的结果[2.19].根据 Langmuir模型计算出FeMnNi-LDHs 对As(\blacksquare)在25、35和45℃条件下的最大平衡吸附量分别为:243.90、250.00和265.16



(a)和(b)吸附前 FeMnNi-LDHs 的 TEM 图像; (c)和(d)吸附后 FeMnNi-LDHs 的 TEM 图像

图 2 吸附As(III)前后 FeMnNi-LDHs 的 TEM 图像

Fig. 2 TEM image of FeMnNi-LDHs before and after the adsorption of As(III)

mg·g⁻¹,略大于实验结果值. 根据 Freundlich 模型拟合计算出不同温度的 n 值均大于 1,说明 FeMnNi-LDHs 对As(\blacksquare)的吸附容易进行,且发生化学吸附过程^[26].

进一步考察 FeMnNi-LDHs 对As(\square)吸附的热力学特性,采用标准吉布斯自由能(ΔG^{θ})、标准焓变(ΔH^{θ})和标准熵变(ΔS^{θ})参数来进行描述. 计算结果如表 2 所示, ΔG^{θ} 为负值表明 FeMnNi-LDHs 对As(\square)的吸附过程是自发进行的, ΔH^{θ} 为正值表明吸附过程是吸热过程, ΔS^{θ} 为正值表明吸附过程为熵推动过程 \square

为了探究As(Ⅲ)在 FeMnNi-LDHs 上的吸附机制,测定了吸附后溶液中的 Cl⁻的浓度增加量,如图4所示,溶液中的Cl⁻随着As(Ⅲ)吸附量的升高逐渐升高,呈现正相关关系,表明 FeMnNi-LDHs 在吸附As(Ⅲ)的同时向溶液中释放了部分Cl⁻.溶液中

的 Cl⁻来源于 FeMnNi-LDHs 层间阴离子,层间阴离子与板层金属离子存在着较弱的化学键,当溶液中

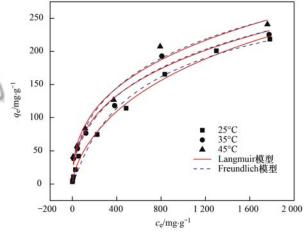


图 3 FeMnNi-LDHs 对 As(III)的等温吸附曲线及拟合

Fig. 3 Isothermal adsorption curve and fitting of FeMnNi-LDHs for As(Ⅲ)

表 1 FeMnNi-LDHs 吸附 As(III) 等温吸附模型相关参数

Table 1	Parameters of	the isothermal	adsorption	model for	FeMnNi-LDHs	adsorption	As(I I)	
---------	---------------	----------------	------------	-----------	-------------	------------	------------------	--

	实验测试		Langmuir 模型			Freundlich 模型	
温度/℃	最大吸附量 /mg·g ⁻¹	$Q_{ m max}$ $/{ m mg} \cdot { m g}^{-1}$	$K_{ m L}$ /L·mg ⁻¹	R^2	n	$K_{\rm F}$ /(mg·g ⁻¹)·(mg·L) ⁻ⁿ	R^2
25	218. 39	243. 90	0.0033	0. 954	1. 625	1. 505	0. 992
35	225. 35	250.00	0.0044	0. 969	2. 689	3. 140	0. 979
45	240. 86	265. 16	0.0049	0. 970	2. 836 0	3. 429	0. 974

表 2 FeMnNi-LDHs 吸附 As(Ⅲ)热力学相关参数

Table 2 FeMnNi-LDHs adsorption As(III) thermodynamic related parameters

T/K	${\rm ln}k_{ m d}$	$\Delta G^{\theta}/\mathrm{kJ}\cdot\mathrm{mol}^{-1}$	$\Delta H^{\theta}/\mathrm{kJ \cdot mol^{-1}}$	$\Delta S^{\theta}/J \cdot (\bmod \cdot K)^{-1}$	R^2
298. 15	8. 10	- 20. 08	15. 66	120. 11	0. 944
308. 15	8. 39	-21.49	15.66	120. 11	0. 944
318. 15	8. 50	- 22. 26	15.66	120. 11	0. 944

阴离子浓度远大于层间阴离子浓度时,由于竞争吸 附,层间阴离子很容易断开旧键,重新结合溶液中的 阴离子. 而在 pH 为 5.5 ± 0.1 范围内, As(Ⅲ)主要 以电中性的 H, AsO, 形态存在[28], 无法水解出阴离 子,电中性的 H, AsO, 扩散至固液界面,通过与材料 表面羟基形成单齿或多齿的络合物而被吸附到材料 上,Mn(IV)具有较强的氧化能力,将材料表面和溶 液中部分As(Ⅲ)氧化为As(V),还原生成的 Mn²⁺ 易溶解,材料表面的部分As(V)随 Mn2+的溶解脱 附进入溶液^[29],溶液中的As(V)在实验 pH 范围内 发生水解反应,最终以 H,AsO4 和 HAsO4 的形态 存在[28],并且在吸附后的溶液中和 XPS 表征结果均 显示有As(V)存在. 吸附后溶液中的 Cl 增加量明 显比 As(Ⅲ) 的吸附量高,可能是 H,AsO₄ 和 $HAsO_4^2$ 与 Cl 产生离子交换同时,溶液中的 CO_3^2 也与 Cl⁻进行了交换,吸附As(Ⅲ)后材料的 FT-IR 图谱也显示出了明显的 CO₃²⁻ 的特征峰.

为了评价 FeMnNi-LDHs 对As(Ⅲ)的优异吸附效果,将该材料与其他研究者制备的层状双氢氧化物进行了比较. 如表 3 所示,相较于 FeMg-LDHs、MgAl-LDHs 和 ZnAl-LDHs 等层状双氢氧化物,本研究制备的FeMnNi-LDHs对As(Ⅲ)具有较高的吸附

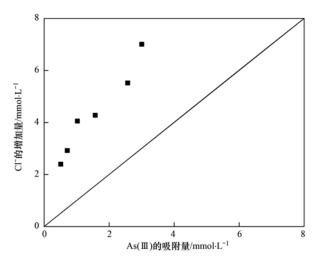


图 4 吸附平衡时溶液中 Cl-浓度与As(Ⅲ)吸附量的关系

Fig. 4 Relationship between Cl⁻ concentrations and the As(III) adsorption capacity in a solution at adsorption equilibrium

性能,这可能是因为 FeMnNi-LDHs 具有氧化性,可以将部分溶液中的 As(III) 氧化成 As(V),改变 As(III) 的存在形态,实现层间离子交换吸附 As(III).并且在氧化As(III)的同时伴随着 Mn^{2+} 的溶解, Mn^{2+} 的脱落为As(III)提供了更多的吸附位点,从而增强了层状双氢氧化物对As(IIII)的吸附能力.

表 3 层状双氢氧化物材料对 As 吸附性能比较

	1 7 11	/ 0	/ \	1.00	
Table 2	Commoniana of A	a adametica	properties of lavered	l dandala buduanida	. mastaniala
Table 5	Comparison of A	s adsorption	properties of favered	i agubie nyaroxiae	materiais

吸附剂	吸附质	吸附质质量浓度/mg·L-1	最大吸附量/mg·g ⁻¹	文献
FeMnNi-LDHs	As(III)	0 ~ 2 000	240. 86	本研究
MgAl-LDHs	As(V)	0 ~ 200	102. 90	[13]
CoAl-LDHs@ boehmite	As(V)	3. 5 ~ 200	38. 50	[14]
$\gamma\text{-Fe}_2\text{O}_3\text{-Mg/Al-LDHs}$	As(V)	7. 5 ~ 1 875	90. 60	[16]
$\mathrm{Fe_3O_4@Al_2O_3@Zn\text{-}Fe\text{-}LDHs}$	As(V)	10 ~ 300	67. 57	[30]
MgAl-LDHs	As(V)	0 ~ 7 500	142. 86	[31]
ZnAl-LDHs	As(III)和As(V)	7.5 ~75	As(\mathbb{II}): 34.24; As(\mathbb{V}): 47.39	[32]

2.3 吸附动力学实验

吸附速率是影响吸附动力学的重要特征,不同的As(Ⅲ)初始质量浓度下材料的吸附动力学曲线如图 5 所示. 在As(Ⅲ)初始质量浓度为 50、20 和10 mg·L⁻¹时,材料在前 4 h 内吸附量显著增加,吸附速率较快,随着时间的延长,吸附速率逐渐变缓,并在 8 h 左右达到吸附平衡,最终去除率分别可达69.54%、76.34%和 82.04%.

分别采用了准一级动力学模型和准二级动力学模型对吸附动力学过程进行了拟合,拟合结果如图 5 和表 4. 两种动力学模型均能较好地拟合吸附动力学过程,但相较于准一级动力学模型,准二级动力学模型能更好地描述 FeMnNi-LDHs 对As(Ⅲ)的吸附

过程,并且拟合出的平衡吸附量更接近实验结果,表明 FeMnNi-LDHs 对As(\blacksquare)的吸附更满足化学吸附机制 $^{[33]}$.此外,在初始质量浓度为 50 mg·L $^{-1}$ 时,准二级动力学模型的速率常数 k_1 为 0.087 0 g·(mg·h) $^{-1}$,表明 FeMnNi-LDHs 在As(\blacksquare)浓度较高时仍具有较快地吸附速率,并能在较短时间内达到平衡,相比于其它报道的同类型的层状双氢氧化物材料,如 Kang等 $^{[11]}$ 制备出的 MgFe-LDHs 在As(V) 初始质量浓度为 50 mg·L $^{-1}$ 时,吸附速率常数为 0.011 3 g·(mg·h) $^{-1}$; Guo等 $^{[34]}$ 制备出的FeMg-LDHs 在As(\blacksquare) 初始质量浓度为 7.5 mg·L $^{-1}$ 时,吸附速率常数0.000 3 g·(mg·h) $^{-1}$,本研究制备出的FeMnNi-LDHs 对As(\blacksquare) 吸附具有较高的速率.

·参数
i

Table 4	Fitting	narameters of	masi-fi	rst-order	and	quasi-second	-order	kinetic r	nodels

不同处理 (c_0)	实验测定值 q_e	Y	生一级动力学模型	Ā		准二级动力学模型	
$/\mathrm{mg} \cdot \mathrm{L}^{-1}$	/mg•g ⁻¹	$q_{\rm e}/{ m mg}\cdot{ m g}^{-1}$	k_1 / h $^{-1}$	R^2	$q_{\rm e}/{\rm mg}\cdot{\rm g}^{-1}$	$k_2/g \cdot (\text{mg} \cdot \text{h})^{-1}$	R^2
50	34. 77	33. 89	2. 62	0. 994	35. 33	0. 087	0. 999
20	15. 27	14. 98	1. 29	0.890	15. 33	0. 159	0. 978
10	8. 20	7. 88	1.81	0. 945	8. 26	0.310	0. 981

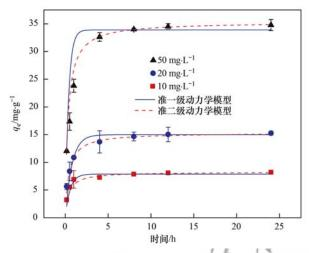


图 5 不同初始浓度下 FeMnNi-LDHs 对 As(Ⅲ)的 吸附动力学拟合

Fig. 5 Kinetic fitting of the adsorption of As(III) by FeMnNi-LDHs at different initial concentrations

2.4 pH 对吸附的影响

溶液 pH 对材料的吸附性能有着重大的影响,它不仅影响吸附质在溶液中的赋存形态,还会影响材料表面的带电性质. 不同 pH 对 FeMnNi-LDHs 吸附As(Ⅲ)的影响如图 6 所示,随着 pH 的升高材料吸附量总体呈现下降趋势. 当溶液 pH 为 2 时,材料

有最大吸附量:15.796 mg·g⁻¹,此时溶液中 Ni²⁺和 Mn2+含量较高,材料在较低 pH 下发生了部分溶解, 而溶解出的 Fe3+、Mn2+和 Ni2+易与砷产生絮凝作 用,使溶液中部分As(Ⅲ)通过沉降作用吸附在材料 表面,因此增加了材料对As(Ⅲ)的吸附量^[22].采用 Zata 电位仪[35]测得 FeMnNi-LDHs 的零点电位 pH.... = 7.17. 当溶液 pH 在 3~9 范围内时,材料对 As(Ⅲ)均有较好的吸附能力,且随 pH 变化较小,此 时溶液中的As(Ⅲ)主要以电中性的 H,AsO,形态存 在,FeMnNi-LDHs 对As(Ⅲ)的吸附主要为表面络合 作用[36],其中 Fe3+、Ni2+和 Mn2+溶出率均小于 4%,表明材料在 pH 在 3~9 范围内有较好的稳定 性. 当 pH > 9 时,溶液中的 H,AsO, 开始解离为 H₂AsO₃⁻、HAsO₃²⁻和AsO₃³⁻,材料表面带负电荷,溶 液中的阴离子与材料产生静电排斥作用,从而使得 材料对As(Ⅲ)的吸附量明显降低[37],此时材料中 Fe 几乎不溶出, Mn2+和 Ni2+溶出率小于 3%. 因此, 可以总结出 FeMnNi-LDHs 材料在溶液 pH > 3 时,均 具有良好的稳定性. 吸附后溶液的 pH 相较于初始 pH 发生了一定的变化,测得材料的等电点 pH_{pre} = 7.17, 当 pH ≤ 7 时, 吸附后溶液 pH 均大于初始 pH, 这可能是因为砷酸根和亚砷酸根离子通过替换材料

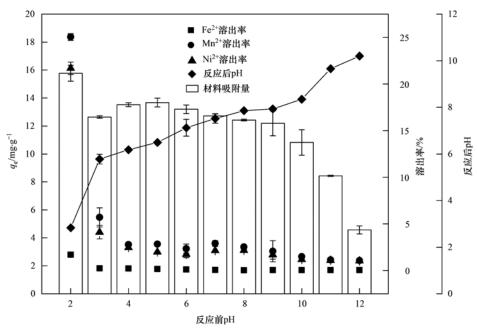


图 6 pH 对 FeMnNi-LDHs 吸附 As(III)的影响及材料溶出情况

Fig. 6 Effect of pH on the adsorption of FeMnNi-LDHs As(III) and the dissolution of materials

表面的—OH 向溶液中释放了 OH ⁻ 所致,说明材料在吸附As(Ⅲ)过程中存在着配体交换^[27]. 然而,当pH > 7 时,吸附后溶液 pH 均有所降低,这可能是 As 与材料表面金属形成了配合物: Fe—O—As、Mn—O—As和 Ni—O—As,并释放了H^{+[38]}. 其它吸附剂在吸附 As(Ⅲ)后, pH 也发生了类似的变化^[28].

测定了吸附后溶液中不同价态的 As 含量,如图 7 所示,吸附后溶液中的As(Ⅲ)和As(Ⅴ)进行了相 互转化, 当 pH 为 2 时, 转化率最高, 其中有 68.00% 的As(Ⅲ)转化为了As(V),这可能是材料中部分 Mn 在制备过程中氧化为 Mn(Ⅳ), 在低 pH 环境下 溶出较多,Mn(IV)具有较强的氧化性,将溶液中的 部分As(Ⅲ)氧化为了As(Ⅵ). As(Ⅲ)的转化率总 体随着 pH 的升高而降低,在 pH 为 3~9 范围内变 化较为平稳,当 pH > 9 时,其转化率明显下降,跟溶 液中 Mn 的溶出率几乎存在着相同的变化趋势,并 且 Zhou 等^[17]制备的 FeMnMg-LDH 在 pH 为 3.5~6 范围内吸附 Pb2+后,材料中的 Mn 溶出率几乎为 0%, 更表明 Mn 的溶出与溶液中As(Ⅲ) 的转化有着 直接联系,这与 Yin 等[29] 的报道一致,可能是 FeMnNi-LDHs 中的 Mn(IV)将吸附到材料表面和部 分溶液中的As(Ⅲ)氧化成了As(V),还原生成的 Mn^{2+} 易从材料中溶出,材料表面的As(V) 随着 Mn2+的溶解进入了溶液,因此 FeMnNi-LDHs 可将-部分毒性较高的As(Ⅲ)转化为毒性较低的As(V), 可有效控制As(Ⅲ)的毒性.

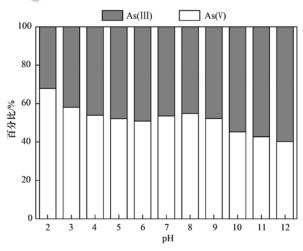


图 7 pH 对As(III)和As(V)转化率的影响

Fig. 7 The pH effect on As(III) and As(V) conversion

2.5 竞争离子对吸附的影响

自然水体水质复杂,往往存在着多种离子的相互影响,因此本研究选取了水体中常见的 5 种离子: NO_3^- 、 PO_4^{3-} 、 CO_3^{2-} 、 Cd^{2+} 和 Pb^{2+} 来探究竞争离子对材料吸附 As(III) 的影响,结果如图 8 所示. 当

NO₃ 质量浓度从 0 增加到 100 mg·L⁻¹时, FeMnNi-LDHs 对As(Ⅲ)的平衡吸附量仅有微弱的变化,降 低幅度均小于 5 mg·g-1, 表明 NO; 的共存对 FeMnNi-LDHs 吸附As(Ⅲ)影响较小,与胡艳玲[36] 的研究结果一致,这是因为 NO。与 LDHs 材料的亲 和力小于被氧化生成的砷酸根离子与材料的亲和 力. 当 PO₄ - 质量浓度从 0 mg·L⁻¹ 增加到 100 mg·L⁻¹时,FeMnNi-LDHs 对As(Ⅲ)的平衡吸附量从 35.43 mg·g⁻¹ 降低至了 14.76 mg·g⁻¹,降低了 58.34%,下降幅度较为明显.这可能是由于磷和砷 属于同一族元素,具有相似的结构,可以与材料表面 的羟基结合形成络合物,部分磷酸根竞争了As(Ⅲ) 在 FeMnNi-LDHs 表面的吸附位点,此外,PO4 具有 更强的置换作用,可以将 FeMnNi-LDHs 表面或内层 已经络合的砷含氧阴根离子置换出来[38]. 随着 CO₃ 质量浓度的增加 FeMnNi-LDHs 对As(Ⅲ)的吸 附平衡量总体呈现降低的趋势,其平衡吸附量由 35.43 mg·g⁻¹ 降低至了 20.63 mg·g⁻¹,降低了 41.76%,相较于 PO₄ 的影响减弱. 这可能是由于溶 液 pH 为 5.5, 部分 CO₃²⁻ 发生水解, 以 HCO₅ 的形 式存在,与溶液中的砷酸根离子形成了竞争吸附,相 较于砷酸根离子,HCO;能更快更多地占据材料的 吸附位点,并与其上的羟基铁氧化物形成更稳定的 表面络合物[39]. 随着 Cd2+ 和 Pb2+ 浓度的增加, FeMnNi-LDHs 对As(Ⅲ)吸附量总体呈现下降趋势, 但变化不大(介于30.68 mg·g⁻¹和35.42 mg·g⁻¹之 间),均具有较好的吸附效果,表明 Cd2+ 和 Pb2+ 对 As(Ⅲ)的吸附竞争较小,这可能是因为 FeMnNi-LDHs 对As(Ⅲ)和 Cd2+和 Pb2+存在着不同的吸附 机制, FeMnNi-LDHs 对 Cd2+和 Pb2+的吸附主要表 现为同构替代和表面沉淀,对As(Ⅲ)的吸附主要表 现为络合和层间离子交换,阳离子 Cd2+和 Pb2+对 As(Ⅲ)的吸附位点影响较小,因此竞争吸附小^[40].

2.6 吸附机制分析

为了进一步讨论材料和吸附质之间的作用机制,对吸附前后的材料进行了表征分析. FeMnNi-LDHs 吸附As(Ⅲ)前后的 FTIR 图谱如图 9 所示. 在 3 400 cm ⁻¹和1 630 cm ⁻¹附近出现的较宽的吸收峰分别是 O—H 和 H₂O 收缩振动峰,表示材料层间水分子和表面吸附水,吸附后 O—H 主峰强度明显升高,表明吸附过程中有大量的层间水分子生成,这可能是砷酸根离子与层板上的羟基发生了反应,从而产生了层间水^[41]. 在1 358 cm ⁻¹处出现的强吸收峰为 O—C—O 的伸缩振动峰,材料吸附As(Ⅲ)后该伸缩振动峰强度明显增大,可能是吸附过程中由于没有严格控制在无氧环境,空气中 CO₂ 融入水中形

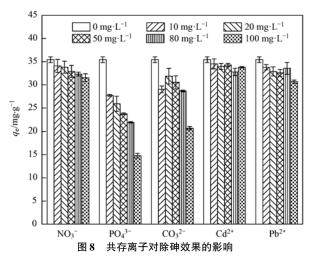


Fig. 8 Effect of co-existing ions on arsenic removal

成 CO₃²-,水中的 CO₃² 与As(Ⅲ)形成竞争吸附,进入层板间与 Cl⁻进行了交换^[42],这与图 4 结果一致. 材料吸附As(Ⅲ)后在 770 cm⁻¹处出现了一个新的特征峰,据报道,该峰为 As—O 的伸缩振动峰^[43],说明溶液中的 As(Ⅲ)被成功吸附到了FeMnNi-LDHs 上. 664 cm⁻¹和 490 cm⁻¹左右的强吸收峰为层状双氢氧化物骨架金属 M—O 的收缩振动峰,与吸附前相比,吸附后主峰强度发生了不同程度的增加和偏移,这可能是As(Ⅲ)与层板上的 M—O 发生了配位络合反应^[44].

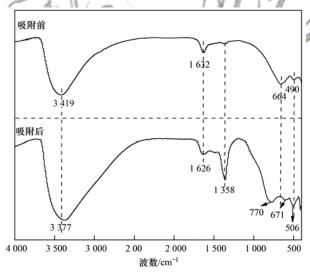


图 9 FeMnNi-LDHs 对 As(III) 吸附前后的 FT-IR 图谱

Fig. 9 FT-IR mapping of FeMnNi-LDHs before and after As(III) adsorption

采用 XPS 进一步探究了 FeMnNi-LDHs 吸附 As(Ⅲ)前后各元素价态和含量的变化,其表征拟合结果如图 10 和表 5 所示. 图 10(a)为吸附前后 Cl元素变化情况,材料吸附后该特征峰下降明显,几乎完全消失,说明层间 Cl⁻与溶液中氧化生成砷酸根离子进行了交换,被吸附到了材料层间. 图 10(b)为 FeMnNi-LDHs 吸附 As(Ⅲ)前后的 O 1s 轨道拟合

峰,该峰在结合能 530. 8、531. 5 和 532. 5 eV 处可分为 3 个峰,分别代表了晶格氧 M—0、羟基—OH 和吸附水 H₂O^[45],吸附 As(Ⅲ)后材料中的 M—O 和—OH分别减少了 19. 08% 和 13. 08%,而 H₂O 增加了 2. 29%,并且在结合能 531. 2 eV 处出现了一个新的 As—O 特征峰. M—O、—OH 含量的减少和 As—O的出现说明溶液中的 As 可能是通过取代材料层板上的—OH 形成表面络合物而被吸附^[46],这与 FT-IR 表征结果—致.

图 10(c) 为吸附前后 FeMnNi-LDHs 的 Fe 2p 轨道的拟合峰. 在 FeMnNi-LDHs 中, Fe $2p_{3/2}$ 和 Fe $2p_{1/2}$ 峰主要集中在 726. 2 和 712. 6 eV,表明材料中的 Fe 元素主要以 Fe(II)的 FeOOH 和 Fe₂O₃ 形态存在^[47]. 而吸附后的 FeMnNi-LDHs 在结合能 710. 5 eV 处出现了一个新 Fe(II)的拟合峰,该峰峰面积小,约占 5. 34%,说明在吸附过程中有少部分的 Fe(III)被还原成了 Fe(II).

图 10(d) 为吸附前后 Mn 2p 轨道的拟合峰,吸附前后的 FeMnNi-LDHs 在结合能为 641.9 和 644.1 eV 处有均有拟合峰,该峰分别表示 Mn(II) 和 $Mn(IV)^{[48]}$,吸附后两峰发生了明显的变化,其中 Mn(IV) 含量由 67.14% 下降到了 42.03%,说明 Mn(IV) 参与了As(III) 氧化成As(V) 的过程.

图 10(e) 为吸附前后 Ni 2p 轨道拟合峰,其中在结合能 855. 8、873. 1、856. 8 和 874. 5 eV 处的拟合峰分别表示 Ni 在材料中主要以 Ni(OH)₂、NiOOH和 NiO 形态存在^[49],表明 Ni 主要以羟基化合物形式存在,易与 As(III)络合形成表面配合物 Ni—O—As,为As(III)提供了较多的吸附位点. 吸附后材料中的 Ni $2p_{3/2}$ 峰向低结合能方向移动,说明部分 Ni 在吸附过程中发生了还原反应,参与了 As(III)氧化成As(V)的过程. Ni 的存在不仅提供了更多的吸附位点,并且参与了氧化,在As(III)的吸附过程中有着重要作用.

图 10(f) 为吸附后的 As 3d 轨道拟合峰,在结合能为 $45.2\,eV$ 和 $44.2\,eV$ 处的拟合峰分别代表了 As(V) 和 $As(III)^{[50]}$,FeMnNi-LDHs 吸附的 As 中有 46.71% 的 As(III) 和 53.29% 的 As(V),表明在吸附过程中有部分的 As(III) 发生了氧化反应,这可能是由于板层上的 Fe、Mn 和 Ni 从吸附到材料表面和溶液中的 As(III) 夺得电子,被还原成低价态的 Fe(III)、Mn(III) 和 Ni(III),而As(IIII) 被氧化成了高价态的 As(V). 其中相较于 Fe 和 Ni,Mn 在 As(IIII) 的氧化过程中起到了主要作用,与已有报道一致 Isometric 100% 。层板上 Isometric 100% 的吸附可用以下方程式 Isometric 200% 。

$$Mn(IV) + H_3AsO_3 + H_2O \longrightarrow$$

$$Mn(II) + H_3AsO_4 + 2H^+ \qquad (2)$$

$$MOOH + H_3AsO_3 \longrightarrow M \longrightarrow O \longrightarrow H_2AsO_3 + H_2O \qquad (3)$$

$$MOOH + H_2AsO_4^- \longrightarrow M \longrightarrow O \longrightarrow HAsO_4 + H_2O \qquad (4)$$

式中,MOOH 表示金属元素 Fe、Mn 和 Ni 的羟基化合物, $M—O—H_2AsO_3$ 和 $M—O—HAsO_4$ 分别表示亚砷酸和砷酸根离子与层板金属 Fe、Mn 和 Ni 形成的配合物.

综上所述,FeMnNi-LDHs 对As(\blacksquare) 的吸附是一个较为复杂的过程,其吸附机制可能包括 2 个方面 (如图 11) :①FeMnNi-LDHs 层板上的 Mn(\blacksquare) 通过电子转移直接将溶液中的部分 As(\blacksquare) 氧化为 As(\blacksquare) 入As(\blacksquare) 水解产生 \blacksquare 2AsO $^-$ 和 \blacksquare HAsO 2 ,与 FeMnNi-LDHs 层间 \blacksquare 2Cl 进行离子交换被吸附到材料层间或者通过与层板羟基结合形成表面配合物而被吸附 \blacksquare 52.54 .②As(\blacksquare) 首先通过扩散迁移至固液界面,通过形成单齿和多齿配合物被吸附到材料表面. 其次,FeMnNi-LDHs 层板上的 Mn(\blacksquare) 发生电子转

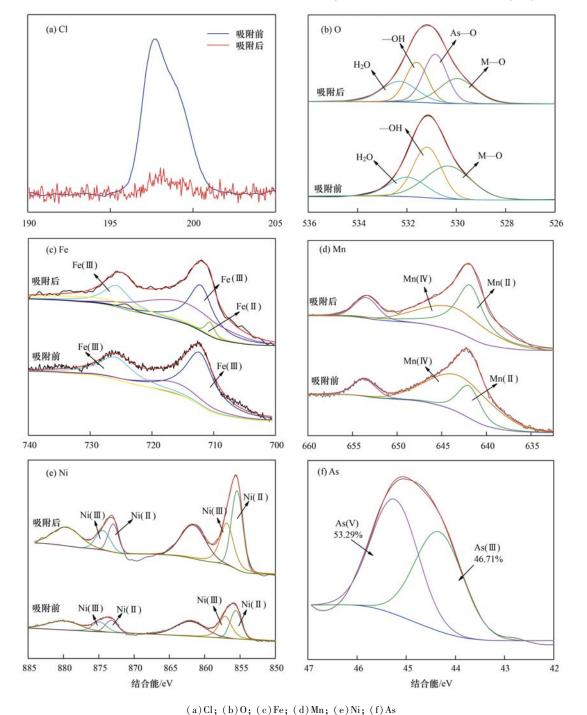


图 10 FeMnNi-LDHs 对As(III) 吸附前后的 XPS 图谱

Fig. 10 XPS patterns of FeMnNi-LDHs before and after As(III) adsorption

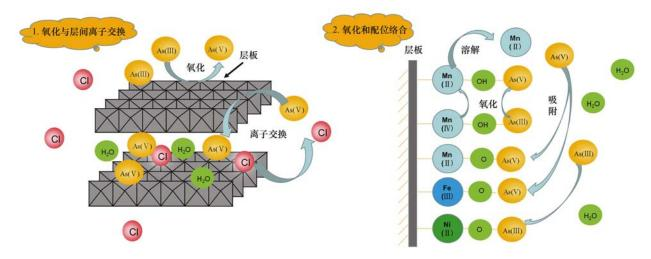


图 11 FeMnNi-LDHs 对As(III)的吸附机制

Fig. 11 Adsorption mechanism of As(III) by FeMnNi-LDHs

表 5 吸附 As(III)前后 FeMnNi-LDHs 上各元素价态和含量变化

Table 5 Changes in the valence and content of each element

on the FeMnNi-LDHs before and after As(III) adsorption

项目	吸附前元素 质量分数/%	吸附后元素 质量分数/%	吸附前后 变化量/%
—ОН	38. 65	25. 57	13. 08
H_2O	19. 36	21. 65	2. 29
M-O	41. 98	22. 90	19.08
As—O	(0) 1	29. 87	29. 87
Fe(II)	-0/	5. 34	5. 34
Fe(II)	100	94. 66	5. 34
Mn(II)	32. 86	57. 97	25. 11//
Mn(IV)	67. 14	42. 03	25. 11
Ni(II)	48. 18	54. 97	6.79
Ni(III)	51. 81	45. 03	6. 79
As(III)	100	46. 71	53. 29
As(V)	0	53. 29	53. 29

移将材料表面的As(Ⅲ)氧化成As(V),随着 Mn²⁺ 的还原溶解,材料表面的As(V)被释放到溶液中, 水解产生 H₂AsO₄ 和 HAsO₄ -,与 FeMnNi-LDHs 层 间 Cl - 进行离子交换重新被吸附到材料层间,进入 溶液的部分 Mn2+会再次被吸附到材料表面,被溶解 氧氧化成 MnO₂^[55,56]. 最后溶液中部分As(V) 和未 被氧化的As(Ⅲ)通过取代层板 M—OH(M 为金属 元素 Fe、Mn 和 Ni)形成 M—O—H₂AsO₃和 M—O—HAsO₄表面配合物而被吸附. 因此 FeMnNi-LDHs 对As(Ⅲ)的吸附机制包含了:氧化、离子交换 和配位络合反应. 其中 Mn 在吸附过程中主要起到 了氧化的作用,可将溶液中的As(Ⅲ)氧化成 As(V),改变了 As 在溶液中的存在形态,相较于普 通的层状双氢氧化物,Mn 的存在大大增加了其对 As(Ⅲ)的吸附效果. Fe 主要起到了吸附作用,可以 高效地吸附氧化生成的As(V) 和部分未被氧化的 As(Ⅲ). Ni 的存在,加强了材料稳定性,使吸附后的 材料仍能保持良好的层状结构,大大提高了材料的重复使用率,Ni表面含有大量羟基,为As提供了更多的吸附位点,也参与了As(Ⅲ)的氧化,对As(Ⅲ)的吸附有着重要作用.

本研究制备出的 FeMnNi-LDHs 可通过氧化作用改变As(III)在溶液中的形态,使得一部分As(III)可通过离子交换被吸附,并且随着 Mn²+的溶解,为As(III)提供了更多的吸附位点,大大增加了As(III)的吸附效果. 较于普通的层状双氢氧化物,FeMnNi-LDHs 对As(III)有良好的吸附效果,且有效地控制了As(III)的毒性,在环境修复领域具有较大的潜力.

3 结论

- (1)本研究在金属量比 Fe: Mn: Ni = 1: 1: 2条件下,采用共沉淀法制备出了 FeMnNi-LDHs 材料,采用 XRD 和 TEM 进行表征显示制备出的 FeMnNi-LDHs 具有层状双氢氧化物的特征峰和典型的层状结构.
- (2)将 FeMnNi-LDHs 用于吸附水中As(Ⅲ),其等温吸附曲线和动力学曲线分别更符合 Freundlich等温吸附模型和准二级动力学模型, FeMnNi-LDHs 对As(Ⅲ)的吸附主要为化学吸附. 45℃时 FeMnNi-LDHs 对As(Ⅲ)的最大吸附量为 240. 86 mg·L⁻¹,在 pH 为 2~9 范围内,材料对As(Ⅲ)均有较好的吸附效果. PO₄³⁻ 和 CO₃²⁻ 对材料吸附As(Ⅲ)存在着竞争吸附,而 NO₃⁻、Cd²⁺、Pb²⁺对吸附影响较小.
- (3) FeMnNi-LDHs 对As(Ⅲ)的吸附机制包括:氧化、离子交换、配位络合, Mn 对As(Ⅲ)的氧化改变了As(Ⅲ)在溶液中的存在形态,大大提升了材料对As(Ⅲ)的吸附效果, Ni 的存在增强了材料稳定性. 总体来说, FeMnNi-LDHs 制备过程简单、成本

低,可以同时实现对As(III)的氧化和吸附,有效控制了水中As(III)的毒性,在水处理和环境修复中具有良好的应用前景.

参考文献:

- [1] 胡志刚, 臧文超, 王玉, 等. 西南地区砷渣堆场周边地下水 污染与防控对策[J]. 环境与可持续发展, 2018, **43**(2): 98-100.
 - Hu Z G, Zang W C, Wang Y, et al. The measures to control groundwater pollution around the arsenic slag in Southwest China [J]. Environment and Sustainable Development, 2018, 43(2): 98-100.
- [2] 曾辉平, 吕塞塞, 杨航, 等. 铁锰泥除砷颗粒吸附剂对As(V)的吸附去除[J]. 环境科学, 2018, **39**(1): 170-178. Zeng H P, Lü S S, Yang H, *et al.* Arsenic(V) removal by granular adsorbents made from backwashing residuals from biofilters for iron and manganese removal [J]. Environmental Science, 2018, **39**(1): 170-178.
- [3] Saxena V K, Kumar S, Singh V S. Occurrence, behaviour and speciation of arsenic in groundwater [J]. Current Science, 2004, 86(2): 281-284.
- [4] Makris K C, Sarkar D, Parsons J G, et al. X-ray absorption spectroscopy as a tool investigating arsenic (III) and arsenic (V) sorption by an aluminum-based drinking-water treatment residual [J]. Journal of Hazardous Materials, 2009, 171 (1-3): 980-986.
- [5] Meng X G, Bang S, Korfiatis G P. Effects of silicate, sulfate, and carbonate on arsenic removal by ferric chloride [J]. Water Research, 2000, 34(4): 1255-1261.
- [6] An B, Steinwinder TR, Zhao DY. Selective removal of arsenate from drinking water using a polymeric ligand exchanger [J]. Water Research, 2005, 39(20): 4993-5004.
- [7] Vrijenhoek E M, Waypa J J. Arsenic removal from drinking water by a "loose" nanofiltration membrane [J]. Desalination, 2000, 130(3): 265-277.
- [8] Katsoyiannis I A, Zouboulis A I. Application of biological processes for the removal of arsenic from groundwaters [J]. Water Research, 2004, 38(1); 17-26.
- [9] 朝木尔乐格, 冯流, 霍艳霞. 基于石墨烯载体的铁基材料制 备及除砷性能比较[J]. 环境科学, 2013, **34**(10): 3927-3932
 - Chaomuerlege, Feng L, Huo Y X. Comparison of As removal performance by graphene/iron-based material [J]. Environmental Science, 2013, **34**(10): 3927-3932.
- [10] 朱司航, 赵晶晶, 尹英杰, 等. 针铁矿改性生物炭对砷吸附性能[J]. 环境科学, 2019, **40**(6): 2773-2782.

 Zhu S H, Zhao J J, Yin Y J, *et al.* Application of goethite modified biochar for arsenic removal from aqueous solution[J]. Environmental Science, 2019, **40**(6): 2773-2782.
- [11] Kang D J, Yu X L, Tong S R, et al. Performance and mechanism of Mg/Fe layered double hydroxides for fluoride and arsenate removal from aqueous solution [J]. Chemical Engineering Journal, 2013, 228: 731-740.
- [12] Maziarz P, Matusik J, Straczek T, et al. Highly effective magnet-responsive LDH-Fe oxide composite adsorbents for As(V) removal [J]. Chemical Engineering Journal, 2019, 362: 207-216.
- [13] Lee S H, Tanaka M, Takahashi Y, et al. Enhanced adsorption of arsenate and antimonate by calcined Mg/Al layered double hydroxide; investigation of comparative adsorption mechanism by surface characterization [J]. Chemosphere, 2018, 211: 903-

- 911.
- [14] Lee S Y, Jung K W, Choi J W, et al. In situ synthesis of hierarchical cobalt-aluminum layered double hydroxide on boehmite surface for efficient removal of arsenate from aqueous solutions; effects of solution chemistry factors and sorption mechanism[J]. Chemical Engineering Journal, 2019, 368: 914-923.
- [15] Zhang L K, Qin X Q, Tang J S, et al. Review of arsenic geochemical characteristics and its significance on arsenic pollution studies in karst groundwater, Southwest China [J]. Applied Geochemistry, 2017, 77: 80-88.
- [16] Luo Z M, Cao Z, Xu J, et al. Enhanced removal of As(III) / (V) from water by simultaneously supported and stabilized Fe-Mn binary oxide nanohybrids [J]. Chemical Engineering Journal, 2017, 322: 710-721.
- [17] Zhou H G, Jiang Z M, Wei S Q. A new hydrotalcite-like absorbent FeMnMg-LDH and its adsorption capacity for Pb²⁺ ions in water[J]. Applied Clay Science, 2018, 153: 29-37.
- [18] Lv Z M, Yang S M, Zhu H S, et al. Highly efficient removal of As(V) by using NiAl layered double oxide composites [J]. Applied Surface Science, 2018, 448: 599-608.
- [19] Lu Y, Jiang B, Fang L, et al. High performance NiFe layered double hydroxide for methyl orange dye and Cr(\vec{N}) adsorption [J]. Chemosphere, 2016, 152: 415-422.
- [20] Wang S S, Gao B, Li Y C. Enhanced arsenic removal by biochar modified with nickel (Ni) and manganese (Mn) oxyhydroxides [J]. Journal of Industrial and Engineering Chemistry, 2016, 37: 361-365.
- [21] Wang L Y, Hong J M, Zhang Q, et al. Deciphering highly resistant characteristics to different pHs of oxygen vacancy-rich Fe₂Co₁-LDH/PS system for bisphenol A degradation [J]. Chemical Engineering Journal, 2020, 385: 123620.
- [22] 施惠生,章萍,钱光人,等. 钙铝层状双氢氧化物的改性及表征[J]. 无机化学学报,2010,26(9):1544-1548.
 Shi H S, Zhang P, Qian G R, et al. Hybrid CaAl-SDS-LDH: preparation, structure and intercalation by sodium dodecyl sulfate into tricalcium aluminate (C₃A)[J]. Chinese Journal of inorganic Chemistry, 2010, 26(9):1544-1548.
- [23] Tong D S, Liu M, Li L, et al. Transformation of alunite residuals into layered double hydroxides and oxides for adsorption of acid red G dye[J]. Applied Clay Science, 2012, 70: 1-7.
- [24] Liang X F, Hou W G, Xu Y M, et al. Sorption of lead ion by layered double hydroxide intercalated with diethylenetriaminepentaacetic acid[J]. Colloids and Surfaces A: Physicochemical and Engineering Aspects, 2010, 366 (1-3): 50-57.
- [25] 周宏光. FeMnMg-LDH 的制备及其对环境铅镉污染的钝化效应研究[D]. 重庆: 西南大学, 2017. 46-47.

 Zhou H G. Preparation of FeMnMg layered double hydroxide and its remediation effects on environmental lead and cadmium pollution[D]. Chongqing: Southwest University, 2017. 46-47.
- [26] 吴晴雯, 孟梁, 张志豪, 等. 芦苇秸秆生物炭对水中菲和1, 1-二氯乙烯的吸附特性[J]. 环境科学, 2016, 37(2): 680-688.
 - Wu Q W, Meng L, Zhang Z H, et al. Sorption Characteristics of phenanthrene and 1, 1-dichloroethene onto reed straw biochar in aquatic solutions [J]. Environmental Science, 2016, 37 (2): 680-688.
- [27] Wang J, Kang D J, Yu X L, et al. Synthesis and characterization of Mg-Fe-La trimetal composite as an adsorbent for fluoride removal [J]. Chemical Engineering Journal, 2015,

- **264**: 506-513.
- [28] Vieira B R C, Pintor A M A, Boaventura R A R, et al. Arsenic removal from water using iron-coated seaweeds [J]. Journal of Environmental Management, 2017, 192; 224-233.
- [29] Yin Y W, Zhou T T, Luo H J, et al. Adsorption of arsenic by activated charcoal coated zirconium-manganese nanocomposite; performance and mechanism [J]. Colloids and Surfaces A; Physicochemical and Engineering Aspects, 2019, 575; 318-328.
- [30] Adlnasab L, Shekari N, Maghsodi A. Optimization of arsenic removal with Fe₃O₄ @ Al₂O₃ @ Zn-Fe LDH as a new magnetic nano adsorbent using Box-Behnken design [J]. Journal of Environmental Chemical Engineering, 2019, 7(2): 102974.
- [31] Rahman M T, Kameda T, Kumagai S, et al. Adsorption isotherms and kinetics of arsenic removal from aqueous solution by Mg-Al layered double hydroxide intercalated with nitrate ions [J]. Reaction Kinetics, Mechanisms and Catalysis, 2017, 120 (2): 703-714.
- [32] Bagherifam S, Komarneni S, Lakzian A, et al. Evaluation of Zn-Al-SO₄ layered double hydroxide for the removal of arsenite and arsenate from a simulated soil solution: isotherms and kinetics
 [J]. Applied Clay Science, 2014, 95: 119-125.
- [33] Yang K, Yan L G, Yang Y M, et al. Adsorptive removal of phosphate by Mg-Al and Zn-Al layered double hydroxides; kinetics, isotherms and mechanisms [J]. Separation and Purification Technology, 2014, 124; 36-42.
- [34] Guo Q H, Cao Y W, Zhang Y Q, et al. Effective treatment of arsenic-bearing water by a layered double metal hydroxide: Iowaite[J]. Applied Geochemistry, 2017, 77: 206-212.
- [35] Ociński D, Jacukowicz-Sobala I, Mazur P, et al. Water treatment residuals containing iron and manganese oxides for arsenic removal from water-characterization of physicochemical properties and adsorption studies [J]. Chemical Engineering Journal, 2016, 294: 210-221.
- [36] 胡燕玲. 核壳型稀土掺杂氧化锆的制备及其砷吸附性能研究 [D]. 徐州:中国矿业大学, 2019. 35-36.
- [37] Wang Y Y, Ji H Y, Lu H H, et al. Simultaneous removal of Sb (III) and Cd (II) in water by adsorption onto a MnFe₂O₄-biochar nanocomposite[J]. RSC Advances, 2018, **8**(6): 3264-3273.
- [38] 周晓馨. 铁锰氧化物/介孔氧化硅复合材料对水中砷的吸附性能及机理研究[D]. 杭州: 浙江大学, 2018. 43-44.
- [39] Dong L J, Zinin P V, Cowen J P, et al. Iron coated pottery granules for arsenic removal from drinking water[J]. Journal of Hazardous Materials, 2009, 168(2-3); 626-632.
- [40] Zhang X L, Dou Y K, Gao C G, et al. Removal of Cd(II) by modified maifanite coated with Mg-layered double hydroxides in constructed rapid infiltration systems [J]. Science of the Total Environment, 2019, 685: 951-962.
- [41] Xu W H, Wang J, Wang L, et al. Enhanced arsenic removal from water by hierarchically porous CeO₂-ZrO₂ nanospheres; role of surface-and structure-dependent properties [J]. Journal of Hazardous Materials, 2013, 260: 498-507.
- [42] Tan L C, Wang Y L, Liu Q, et al. Enhanced adsorption of uranium (VI) using a three-dimensional layered double hydroxide/graphene hybrid material [J]. Chemical Engineering Journal, 2015, 259: 752-760.

- [43] Hu X, Ding Z H, Zimmerman A R, et al. Batch and column sorption of arsenic onto iron-impregnated biochar synthesized through hydrolysis [J]. Water Research, 2015, 68: 206-216.
- [44] Dou R Y, Ma J F, Huang D Q, et al. Bisulfite assisted photocatalytic degradation of methylene blue by Ni-Fe-Mn oxide from MnO₄ intercalated LDH[J]. Applied Clay Science, 2018, 161: 235-241.
- [45] Yu Y, Zhang C Y, Yang L M, et al. Cerium oxide modified activated carbon as an efficient and effective adsorbent for rapid uptake of arsenate and arsenite; material development and study of performance and mechanisms [J]. Chemical Engineering Journal, 2017, 315; 630-638.
- [46] Ma L, Cai D M, Tu S X. Arsenite simultaneous sorption and oxidation by natural ferruginous manganese ores with various ratios of Mn/Fe[J]. Chemical Engineering Journal, 2020, 382: 123040.
- [47] Huo Y C, Li W W, Min D, et al. Zero-valent iron nanoparticles with sustained high reductive activity for carbon tetrachloride dechlorination [J]. RSC Advances, 2015, 5 (67): 54497-54504.
- [48] Tan B J, Klabunde K J, Sherwood P M A. XPS studies of solvated metal atom dispersed (SMAD) catalysts. Evidence for layered cobalt-manganese particles on alumina and silica [J]. Journal of the American Chemical Society, 1991, 113(3): 855-861.
- [49] Tian H, Bao W T, Jiang Y, et al. Fabrication of Ni-Al LDH/ Nitramine-N-doped graphene hybrid composites via a novel selfassembly process for hybrid supercapacitors [J]. Chemical Engineering Journal, 2018, 354: 1132-1140.
- [50] Wu L K, Wu H, Zhang H B, et al. Graphene oxide/CuFe₂O₄ foam as an efficient absorbent for arsenic removal from water[J]. Chemical Engineering Journal, 2018, 334: 1808-1819.
- [51] Zheng Q, Hou J T, Hartley W, et al. As(III) adsorption on Fe-Mn binary oxides: are Fe and Mn oxides synergistic or antagonistic for arsenic removal? [J]. Chemical Engineering Journal, 2020, 389: 124470.
- [52] Zhang G S, Liu F D, Liu H J, et al. Respective role of Fe and Mn oxide contents for arsenic sorption in iron and manganese binary oxide: an X-ray absorption spectroscopy investigation[J]. Environmental Science & Technology, 2014, 48 (17): 10316-10322.
- [53] Lin L N, Song Z G, Khan Z H, et al. Enhanced As (III) removal from aqueous solution by Fe-Mn-La-impregnated biochar composites [J]. Science of the Total Environment, 2019, 686: 1185-1193.
- [54] Ren H T, Jia S Y, Wu S H, et al. Abiotic oxidation of Mn(II) induced oxidation and mobilization of As(III) in the presence of magnetite and hematite [J]. Journal of Hazardous Materials, 2013, 254-255: 89-97.
- [55] Chen J, Wang J Y, Zhang G S, et al. Facile fabrication of nanostructured cerium-manganese binary oxide for enhanced arsenite removal from water[J]. Chemical Engineering Journal, 2018, 334: 1518-1526.
- [56] Hou J T, Luo J L, Song S X, et al. The remarkable effect of the coexisting arsenite and arsenate species ratios on arsenic removal by manganese oxide [J]. Chemical Engineering Journal, 2017, 315: 159-166.

HUANJING KEXUE

Environmental Science (monthly)

Vol. 42 No. 1 Jan. 15, 2021

CONTENTS

Concurrent Collection of Ammonia Gas and Aerosol Ammonium in Urban Beijing During National Celebration Days Utilizing an Acid-C	pated Honeycomb Denuder in Combination with a Filter System
	··· GU Meng-na, PAN Yue-peng, SONG Lin-lin, et al. (1)
Heavy Pollution Episode in Tianjin Based on UAV Meteorological Sounding and Numerical Model	
Characteristics and Sources of PM _{2.5} Pollution in Typical Cities of the Central Plains Urban Agglomeration in Autumn and Winter · · ·	MIAO Qing-qing, JIANG Nan, ZHANG Rui-qin, et al. (19)
Characteristics and Sources of Water-soluble Ion Pollution in PM _{2.5} in Winter in Shenyang	· WANG Guo-zhen, REN Wan-hui, YU Xing-na, et al. (30)
Pollution Characteristics and Health Risk Assessment of Heavy Metals in PM _{2.5} Collected in Baoding	LEI Wen-kai, LI Xing-ru, ZHANG Lan, et al. (38)
Source Apportionment of Ambient Carbonyl Compounds Based on a PMF and Source Tracer Ratio Method: A Case Based on Observation	ons in Nanjing
	······ HU Kun, WANG Ming, WANG Hong-li, et al. (45)
Characterization and Source Apportionment of Atmospheric VOCs in Tianjin in 2019	······ GAO Jing-yun, XIAO Zhi-mei, XU Hong, et al. (55)
Characteristics and Source Apportionment of Ambient VOCs in Spring in Liuzhou	
Characteristics of Ozone and Source Apportionment of the Precursor VOCs in Tianjin Suburbs in Summer	LUO Rui-xue, LIU Bao-shuang, LIANG Dan-ni, et al. (75)
Transport Influence and Potential Sources of Ozone Pollution for Nanjing During Spring and Summer in 2017	······ XIE Fang-jian, LU Xiao-bo, YANG Feng, et al. (88)
Ozone Pollution Trend in the Pearl River Delta Region During 2006-2019	
Distribution Characteristics and Source Apportionment of Polycyclic Aromatic Hydrocarbons in Atmospheric Deposition in Areas Adjace	nt to a Large Petrochemical Enterprise · · · · · · · · · · · · · · · · · · ·
25. The state of t	······ LI Da-yan, QI Xiao-bao, WU Jian, et al. (106)
Quantitative Comparison of Methods to Assess the Airborne Particulate Matter Retention Capacity of Leaves	
Emission Estimation and Fate Simulation of Dichlorvos in the Dongjiang River Watershed	··· ZHANG Bing, ZHANG Qian-qian, YING Guang-guo (127)
Distribution and Ecological Risk Assessment of Antibiotics in the Songhua River Basin of the Harbin Section and Ashe River · · · · YA	NG Shang-le, WANG Xu-ming, WANG Wei-hua, et al. (136)
Characteristics and Ecological Risk Assessment of POPs Pollution in Sediments of Xiaoxingkai Lake in the Northeast China	LI Hui, LI Jie, SONG Peng, et al. (147)
Distribution and Ecological Risk Assessment of PPCPs in Drinking Water Sources of Henan Province	····· ZHOU Ying, WU Dong-hai, LU Guang-hua, et al. (159)
Occurrence Characteristics and Health Risk Assessment of Endocrine Disrupting Chemicals in Groundwater in Wuxi-Changzhou	
Seasonal Distribution Characteristics and Health Risk Assessment of Heavy Metals in Surface Water of Qingjiang River	
Metal Pollutions and Human Health Risks in Groundwater from Wet, Normal, and Dry Periods in the Huixian Karst Wetland, China	
Seasonal Variation of DOM Spectral Characteristics of Rivers with Different Urbanization Levels in the Three Gorges Reservoir Area	
Distribution of Micro-plastics in the Soil Covered by Different Vegetation in Yellow River Delta Wetland	
Metagenomic Analysis Provides Insights into Rectarial Communities Antibiotic Resistance and Public Health Risks in the Donoming I	ake Reservoir
neugenome manyon fronces insigne into bacteria communities, Antibote resistones, and Fabre readil rasks in the bongping i	ZHANG Hong-na. CUI Na. SHEN Hong-miao (211)
Mechanism of Algal Community Dynamics Driven by the Seasonal Water Bacterial Community in a Stratified Drinking Water Reservoir	
YAN	Mian-mian ZHANG Hai-han HIJANG Ting-lin et al. (221)
Community Structure, Function, and Influencing Factors of Planktonic Fungi in the Danjiangkou Reservoir	THENG Bao-hai WANG Xiao-vu II Ying-iun et al. (234)
Changes in Algal Particles and Their Water Quality Effects in the Outflow River of Taihu Lake	
Characteristics of Soil Nitrogen and Phosphorus Losses Under Different Land-use Schemes in the Shipanqiu Watershed	
Influence of Antecedent Dry Days on Nitrogen Removal in Bioretention Systems	CHEN Voc. II Vin mi. 7HENC Shuang et al. (263)
Effect of Enteromorpha prolifera Biochar on the Adsorption Characteristics and Adsorption Mechanisms of Ammonia Nitrogen in Rainfall	
Effect of Enteromorphia protifera Diochar on the Adsorption Characteristics and Adsorption Mechanisms of Ammonia Nitrogen in Namian	Kunon
	CHEN Vou vuon II Pai-giong II Vion-obi et al. (274)
	···· CHEN You-yuan, LI Pei-qiang, LI Xian-chi, et al. (274)
Effect of Filter Medium on the Enhancement of Complete Autotrophic Nitrogen Removal over Nitrite Process in a Tidal Flow Constructe	···· CHEN You-yuan, LI Pei-qiang, LI Xian-chi, et al. (274)
Effect of Filter Medium on the Enhancement of Complete Autotrophic Nitrogen Removal over Nitrite Process in a Tidal Flow Constructe	CHEN You-yuan, LI Pei-qiang, LI Xian-chi, et al. (274) d Wetland
Effect of Filter Medium on the Enhancement of Complete Autotrophic Nitrogen Removal over Nitrite Process in a Tidal Flow Constructe Adsorption Effect and Mechanism of Aqueous Arsenic on FeMnNi-LDHs	CHEN You-yuan, LI Pei-qiang, LI Xian-chi, et al. (274) d Wetland LIU Bing, ZHENG Yu-ming, QIN Hui-an, et al. (283) LIAO Yu-mei, YU Jie, WEI Shi-qiang, et al. (293)
Effect of Filter Medium on the Enhancement of Complete Autotrophic Nitrogen Removal over Nitrite Process in a Tidal Flow Constructe Adsorption Effect and Mechanism of Aqueous Arsenic on FeMnNi-LDHs Combined Use of Zirconium-Modified Bentonite Capoing and Calcium Nitrate Addition to Control the Release of Phosphorus from Sedin	CHEN You-yuan, LI Pei-qiang, LI Xian-chi, et al. (274) d Wetland LIU Bing, ZHENG Yu-ming, QIN Hui-an, et al. (283) LIAO Yu-mei, YU Jie, WEI Shi-qiang, et al. (293)
Effect of Filter Medium on the Enhancement of Complete Autotrophic Nitrogen Removal over Nitrite Process in a Tidal Flow Constructe Adsorption Effect and Mechanism of Aqueous Arsenic on FeMnNi-LDHs Combined Use of Zirconium-Modified Bentonite Capping and Calcium Nitrate Addition to Control the Release of Phosphorus from Sedin Distribution Characteristics of Antibiotics and Antibiotic Resistance Genes in Wastewater Treatment Plants	CHEN You-yuan, LI Pei-qiang, LI Xian-chi, et al. (274) d Wetland
Effect of Filter Medium on the Enhancement of Complete Autotrophic Nitrogen Removal over Nitrite Process in a Tidal Flow Constructe Adsorption Effect and Mechanism of Aqueous Arsenic on FeMnNi-LDHs Combined Use of Zirconium-Modified Bentonite Capping and Calcium Nitrate Addition to Control the Release of Phosphorus from Sedin Distribution Characteristics of Antibiotics and Antibiotic Resistance Genes in Wastewater Treatment Plants	CHEN You-yuan, LI Pei-qiang, LI Xian-chi, et al. (274) d Wetland
Effect of Filter Medium on the Enhancement of Complete Autotrophic Nitrogen Removal over Nitrite Process in a Tidal Flow Constructed Adsorption Effect and Mechanism of Aqueous Arsenic on FeMnNi-LDHs Combined Use of Zirconium-Modified Bentonite Capping and Calcium Nitrate Addition to Control the Release of Phosphorus from Sedin Distribution Characteristics of Antibiotics and Antibiotic Resistance Genes in Wastewater Treatment Plants	CHEN You-yuan, LI Pei-qiang, LI Xian-chi, et al. (274) d Wetland
Effect of Filter Medium on the Enhancement of Complete Autotrophic Nitrogen Removal over Nitrite Process in a Tidal Flow Constructed Adsorption Effect and Mechanism of Aqueous Arsenic on FeMnNi-LDHs Combined Use of Zirconium-Modified Bentonite Capping and Calcium Nitrate Addition to Control the Release of Phosphorus from Sedin Distribution Characteristics of Antibiotics and Antibiotic Resistance Genes in Wastewater Treatment Plants	CHEN You-yuan, LI Pei-qiang, LI Xian-chi, et al. (274) d Wetland
Effect of Filter Medium on the Enhancement of Complete Autotrophic Nitrogen Removal over Nitrite Process in a Tidal Flow Constructed Adsorption Effect and Mechanism of Aqueous Arsenic on FeMnNi-LDHs Combined Use of Zirconium-Modified Bentonite Capping and Calcium Nitrate Addition to Control the Release of Phosphorus from Sedin Distribution Characteristics of Antibiotics and Antibiotic Resistance Genes in Wastewater Treatment Plants Occurrence of Antibiotic Resistance Genes and Bacterial Community Structure of Different Sludge Samples During Microwave Pretreatment Plants	CHEN You-yuan, LI Pei-qiang, LI Xian-chi, et al. (274) d Wetland LIU Bing, ZHENG Yu-ming, QIN Hui-an, et al. (283) LIAO Yu-mei, YU Jie, WEI Shi-qiang, et al. (293) nents
Effect of Filter Medium on the Enhancement of Complete Autotrophic Nitrogen Removal over Nitrite Process in a Tidal Flow Constructed Adsorption Effect and Mechanism of Aqueous Arsenic on FeMnNi-LDHs Combined Use of Zirconium-Modified Bentonite Capping and Calcium Nitrate Addition to Control the Release of Phosphorus from Sedin Distribution Characteristics of Antibiotics and Antibiotic Resistance Genes in Wastewater Treatment Plants Occurrence of Antibiotic Resistance Genes and Bacterial Community Structure of Different Sludge Samples During Microwave Pretreatm Selenium Threshold for the Delimitation of Natural Selenium-Enriched Land	CHEN You-yuan, LI Pei-qiang, LI Xian-chi, et al. (274) d Wetland
Effect of Filter Medium on the Enhancement of Complete Autotrophic Nitrogen Removal over Nitrite Process in a Tidal Flow Constructed Adsorption Effect and Mechanism of Aqueous Arsenic on FeMnNi-LDHs Combined Use of Zirconium-Modified Bentonite Capping and Calcium Nitrate Addition to Control the Release of Phosphorus from Sedin 2 Distribution Characteristics of Antibiotics and Antibiotic Resistance Genes in Wastewater Treatment Plants Occurrence of Antibiotic Resistance Genes and Bacterial Community Structure of Different Sludge Samples During Microwave Pretreatm Selenium Threshold for the Delimitation of Natural Selenium-Enriched Land Improved Regression Kriging Prediction of the Spatial Distribution of the Soil Cadmium by Integrating Natural and Human Factors	CHEN You-yuan, LI Pei-qiang, LI Xian-chi, et al. (274) d Wetland
Effect of Filter Medium on the Enhancement of Complete Autotrophic Nitrogen Removal over Nitrite Process in a Tidal Flow Constructed Adsorption Effect and Mechanism of Aqueous Arsenic on FeMnNi-LDHs Combined Use of Zirconium-Modified Bentonite Capping and Calcium Nitrate Addition to Control the Release of Phosphorus from Sedin 2 Distribution Characteristics of Antibiotics and Antibiotic Resistance Genes in Wastewater Treatment Plants Occurrence of Antibiotic Resistance Genes and Bacterial Community Structure of Different Sludge Samples During Microwave Pretreatm Selenium Threshold for the Delimitation of Natural Selenium-Enriched Land Improved Regression Kriging Prediction of the Spatial Distribution of the Soil Cadmium by Integrating Natural and Human Factors Simulation Cadmium (Cd) Accumulation in Typical Paddy Soils in South China	CHEN You-yuan, LI Pei-qiang, LI Xian-chi, et al. (274) d Wetland
Effect of Filter Medium on the Enhancement of Complete Autotrophic Nitrogen Removal over Nitrite Process in a Tidal Flow Constructed Adsorption Effect and Mechanism of Aqueous Arsenic on FeMnNi-LDHs Combined Use of Zirconium-Modified Bentonite Capping and Calcium Nitrate Addition to Control the Release of Phosphorus from Sedin 27 Distribution Characteristics of Antibiotics and Antibiotic Resistance Genes in Wastewater Treatment Plants Occurrence of Antibiotic Resistance Genes and Bacterial Community Structure of Different Sludge Samples During Microwave Pretreatm Selenium Threshold for the Delimitation of Natural Selenium-Enriched Land Improved Regression Kriging Prediction of the Spatial Distribution of the Soil Cadmium by Integrating Natural and Human Factors Simulation Cadmium (Cd) Accumulation in Typical Paddy Soils in South China Bioaccessibility and Health Risks of the Heavy Metals in Soil-Rice System of Southwest Fujian Province	CHEN You-yuan, LI Pei-qiang, LI Xian-chi, et al. (274) d Wetland
Effect of Filter Medium on the Enhancement of Complete Autotrophic Nitrogen Removal over Nitrite Process in a Tidal Flow Constructed Adsorption Effect and Mechanism of Aqueous Arsenic on FeMnNi-LDHs Combined Use of Zirconium-Modified Bentonite Capping and Calcium Nitrate Addition to Control the Release of Phosphorus from Sedin Distribution Characteristics of Antibiotics and Antibiotic Resistance Genes in Wastewater Treatment Plants Occurrence of Antibiotic Resistance Genes and Bacterial Community Structure of Different Sludge Samples During Microwave Pretreatm Selenium Threshold for the Delimitation of Natural Selenium-Enriched Land Improved Regression Kriging Prediction of the Spatial Distribution of the Soil Cadmium by Integrating Natural and Human Factors Simulation Cadmium (Cd) Accumulation in Typical Paddy Soils in South China Bioaccessibility and Health Risks of the Heavy Metals in Soil-Rice System of Southwest Fujian Province Effects of Nano Material on Cadmium Accumulation Capacity and Grain Yield of Indica Hybrid Rice Under Wetting-drving Alternation	CHEN You-yuan, LI Pei-qiang, LI Xian-chi, et al. (274) d Wetland LIU Bing, ZHENG Yu-ming, QIN Hui-an, et al. (283) LIAO Yu-mei, YU Jie, WEI Shi-qiang, et al. (293) nents XIE Ya-wei, YU Chi-sheng, LI Fei-fei, et al. (305) XIE Ya-wei, YU Chi-sheng, LI Fei-fei, et al. (315) ent-Anaerobic Digestion LI Hui-li, WU Cai-yun, TANG An-ping, et al. (323) WANG Hui-yan, ZENG Dao-ming, GUO Zhi-juan, et al. (333) GAO Zhong-yuan, XIAO Rong-bo, WANG Peng, et al. (343) DAI Ya-ting, FU Kai-dao, YANG Yang, et al. (355) LIN Cheng-qi, CAI Yu-hao, HU Gong-ren, et al. (359) Irrigation
Effect of Filter Medium on the Enhancement of Complete Autotrophic Nitrogen Removal over Nitrite Process in a Tidal Flow Constructed Adsorption Effect and Mechanism of Aqueous Arsenic on FeMnNi-LDHs Combined Use of Zirconium-Modified Bentonite Capping and Calcium Nitrate Addition to Control the Release of Phosphorus from Sedin Distribution Characteristics of Antibiotics and Antibiotic Resistance Genes in Wastewater Treatment Plants Occurrence of Antibiotic Resistance Genes and Bacterial Community Structure of Different Sludge Samples During Microwave Pretreatm Selenium Threshold for the Delimitation of Natural Selenium-Enriched Land Improved Regression Kriging Prediction of the Spatial Distribution of the Soil Cadmium by Integrating Natural and Human Factors Simulation Cadmium (Cd) Accumulation in Typical Paddy Soils in South China Bioaccessibility and Health Risks of the Heavy Metals in Soil-Rice System of Southwest Fujian Province Effects of Nano Material on Cadmium Accumulation Capacity and Grain Yield of Indica Hybrid Rice Under Wetting-drying Alternation	
Effect of Filter Medium on the Enhancement of Complete Autotrophic Nitrogen Removal over Nitrite Process in a Tidal Flow Constructed Adsorption Effect and Mechanism of Aqueous Arsenic on FeMnNi-LDHs Combined Use of Zirconium-Modified Bentonite Capping and Calcium Nitrate Addition to Control the Release of Phosphorus from Sedin 27 Distribution Characteristics of Antibiotics and Antibiotic Resistance Genes in Wastewater Treatment Plants Occurrence of Antibiotic Resistance Genes and Bacterial Community Structure of Different Sludge Samples During Microwave Pretreatm Selenium Threshold for the Delimitation of Natural Selenium-Enriched Land Improved Regression Kriging Prediction of the Spatial Distribution of the Soil Cadmium by Integrating Natural and Human Factors Simulation Cadmium (Cd) Accumulation in Typical Paddy Soils in South China Bioaccessibility and Health Risks of the Heavy Metals in Soil-Rice System of Southwest Fujian Province Effects of Nano Material on Cadmium Accumulation Capacity and Grain Yield of Indica Hybrid Rice Under Wetting-drying Alternation Regulation Control of a Tribasic Amendment on the Chemical Fractions of Cd and As in Paddy Soil and Their Accumulation in Rice	
Effect of Filter Medium on the Enhancement of Complete Autotrophic Nitrogen Removal over Nitrite Process in a Tidal Flow Constructed Adsorption Effect and Mechanism of Aqueous Arsenic on FeMnNi-LDHs Combined Use of Zirconium-Modified Bentonite Capping and Calcium Nitrate Addition to Control the Release of Phosphorus from Sedin Distribution Characteristics of Antibiotics and Antibiotic Resistance Genes in Wastewater Treatment Plants Occurrence of Antibiotic Resistance Genes and Bacterial Community Structure of Different Sludge Samples During Microwave Pretreatm Selenium Threshold for the Delimitation of Natural Selenium-Enriched Land Improved Regression Kriging Prediction of the Spatial Distribution of the Soil Cadmium by Integrating Natural and Human Factors Simulation Cadmium (Cd) Accumulation in Typical Paddy Soils in South China Bioaccessibility and Health Risks of the Heavy Metals in Soil-Rice System of Southwest Fujian Province Effects of Nano Material on Cadmium Accumulation Capacity and Grain Yield of Indica Hybrid Rice Under Wetting-drying Alternation Regulation Control of a Tribasic Amendment on the Chemical Fractions of Cd and As in Paddy Soil and Their Accumulation in Rice Combined Effect of Weathered Coal Based Amendments and Soil Water Management on Methylmercury Accumulation in Paddy Soil and	CHEN You-yuan, LI Pei-qiang, LI Xian-chi, et al. (274) d Wetland LIU Bing, ZHENG Yu-ming, QIN Hui-an, et al. (283) LIAO Yu-mei, YU Jie, WEI Shi-qiang, et al. (293) sents XIE Ya-wei, YU Chi-sheng, LI Fei-fei, et al. (305) XIE Ya-wei, YU Chi-sheng, LI Fei-fei, et al. (315) ent-Anaerobic Digestion LI Hui-li, WU Cai-yun, TANG An-ping, et al. (323) WANG Hui-yan, ZENG Dao-ming, GUO Zhi-juan, et al. (333) GAO Zhong-yuan, XIAO Rong-bo, WANG Peng, et al. (343) DAI Ya-ting, FU Kai-dao, YANG Yang, et al. (359) Irrigation YANG Ru, CHEN Xin-rui, ZHANG Ying, et al. (368) YANG Ru, CHEN Xin-rui, ZHANG Ying, et al. (378) I Rice Grains
Effect of Filter Medium on the Enhancement of Complete Autotrophic Nitrogen Removal over Nitrite Process in a Tidal Flow Constructed Adsorption Effect and Mechanism of Aqueous Arsenic on FeMnNi-LDHs Combined Use of Zirconium-Modified Bentonite Capping and Calcium Nitrate Addition to Control the Release of Phosphorus from Sedin Distribution Characteristics of Antibiotics and Antibiotic Resistance Genes in Wastewater Treatment Plants Occurrence of Antibiotic Resistance Genes and Bacterial Community Structure of Different Sludge Samples During Microwave Pretreatm Selenium Threshold for the Delimitation of Natural Selenium-Enriched Land Improved Regression Kriging Prediction of the Spatial Distribution of the Soil Cadmium by Integrating Natural and Human Factors Simulation Cadmium (Cd) Accumulation in Typical Paddy Soils in South China Bioaccessibility and Health Risks of the Heavy Metals in Soil-Rice System of Southwest Fujian Province Effects of Nano Material on Cadmium Accumulation Capacity and Grain Yield of Indica Hybrid Rice Under Wetting-drying Alternation Regulation Control of a Tribasic Amendment on the Chemical Fractions of Cd and As in Paddy Soil and Their Accumulation in Rice Combined Effect of Weathered Coal Based Amendments and Soil Water Management on Methylmercury Accumulation in Paddy Soil and	CHEN You-yuan, LI Pei-qiang, LI Xian-chi, et al. (274) d Wetland
Effect of Filter Medium on the Enhancement of Complete Autotrophic Nitrogen Removal over Nitrite Process in a Tidal Flow Constructed Adsorption Effect and Mechanism of Aqueous Arsenic on FeMnNi-LDHs Combined Use of Zirconium-Modified Bentonite Capping and Calcium Nitrate Addition to Control the Release of Phosphorus from Sedin Distribution Characteristics of Antibiotics and Antibiotic Resistance Genes in Wastewater Treatment Plants Occurrence of Antibiotic Resistance Genes and Bacterial Community Structure of Different Sludge Samples During Microwave Pretreatm Selenium Threshold for the Delimitation of Natural Selenium-Enriched Land Improved Regression Kriging Prediction of the Spatial Distribution of the Soil Cadmium by Integrating Natural and Human Factors Simulation Cadmium (Cd) Accumulation in Typical Paddy Soils in South China Bioaccessibility and Health Risks of the Heavy Metals in Soil-Rice System of Southwest Fujian Province Effects of Nano Material on Cadmium Accumulation Capacity and Grain Yield of Indica Hybrid Rice Under Wetting-drying Alternation Regulation Control of a Tribasic Amendment on the Chemical Fractions of Cd and As in Paddy Soil and Their Accumulation in Rice Combined Effect of Weathered Coal Based Amendments and Soil Water Management on Methylmercury Accumulation in Paddy Soil and Effects of Fertilization Strategies on the Cadmium Resistance of Paddy Soil Microorganisms	CHEN You-yuan, LI Pei-qiang, LI Xian-chi, et al. (274) d Wetland
Effect of Filter Medium on the Enhancement of Complete Autotrophic Nitrogen Removal over Nitrite Process in a Tidal Flow Constructed Adsorption Effect and Mechanism of Aqueous Arsenic on FeMnNi-LDHs Combined Use of Zirconium-Modified Bentonite Capping and Calcium Nitrate Addition to Control the Release of Phosphorus from Sedin Distribution Characteristics of Antibiotics and Antibiotic Resistance Genes in Wastewater Treatment Plants Occurrence of Antibiotic Resistance Genes and Bacterial Community Structure of Different Sludge Samples During Microwave Pretreatm Selenium Threshold for the Delimitation of Natural Selenium-Enriched Land Improved Regression Kriging Prediction of the Spatial Distribution of the Soil Cadmium by Integrating Natural and Human Factors Simulation Cadmium (Cd) Accumulation in Typical Paddy Soils in South China Bioaccessibility and Health Risks of the Heavy Metals in Soil-Rice System of Southwest Fujian Province Effects of Nano Material on Cadmium Accumulation Capacity and Grain Yield of Indica Hybrid Rice Under Wetting-drying Alternation Regulation Control of a Tribasic Amendment on the Chemical Fractions of Cd and As in Paddy Soil and Their Accumulation in Rice Combined Effect of Weathered Coal Based Amendments and Soil Water Management on Methylmercury Accumulation in Paddy Soil and Effects of Fertilization Strategies on the Cadmium Resistance of Paddy Soil Microorganisms Soil Enzyme Activity in Picea schrenkiana and Its Relationship with Environmental Factors in the Tianshan Mountains, Xinjiang	CHEN You-yuan, LI Pei-qiang, LI Xian-chi, et al. (274) d Wetland
Effect of Filter Medium on the Enhancement of Complete Autotrophic Nitrogen Removal over Nitrite Process in a Tidal Flow Constructed Adsorption Effect and Mechanism of Aqueous Arsenic on FeMnNi-LDHs Combined Use of Zirconium-Modified Bentonite Capping and Calcium Nitrate Addition to Control the Release of Phosphorus from Sedin Distribution Characteristics of Antibiotics and Antibiotic Resistance Genes in Wastewater Treatment Plants Occurrence of Antibiotic Resistance Genes and Bacterial Community Structure of Different Sludge Samples During Microwave Pretreatm Selenium Threshold for the Delimitation of Natural Selenium-Enriched Land Improved Regression Kriging Prediction of the Spatial Distribution of the Soil Cadmium by Integrating Natural and Human Factors Simulation Cadmium (Cd) Accumulation in Typical Paddy Soils in South China Bioaccessibility and Health Risks of the Heavy Metals in Soil-Rice System of Southwest Fujian Province Effects of Nano Material on Cadmium Accumulation Capacity and Grain Yield of Indica Hybrid Rice Under Wetting-drying Alternation Regulation Control of a Tribasic Amendment on the Chemical Fractions of Cd and As in Paddy Soil and Their Accumulation in Paddy Soil and Effects of Fertilization Strategies on the Cadmium Resistance of Paddy Soil Microorganisms Soil Enzyme Activity in Picea schrenkiana and Its Relationship with Environmental Factors in the Tianshan Mountains, Xinjiang Effects of Farmland Abandonment on Soil Enzymatic Activity and Enzymatic Stoichiometry in the Loess Hilly Region, China	
Effect of Filter Medium on the Enhancement of Complete Autotrophic Nitrogen Removal over Nitrite Process in a Tidal Flow Constructed Adsorption Effect and Mechanism of Aqueous Arsenic on FeMnNi-LDHs Combined Use of Zirconium-Modified Bentonite Capping and Calcium Nitrate Addition to Control the Release of Phosphorus from Sedin — — — — — — — — — — — — — — — — — — —	CHEN You-yuan, LI Pei-qiang, LI Xian-chi, et al. (274) d Wetland
Effect of Filter Medium on the Enhancement of Complete Autotrophic Nitrogen Removal over Nitrite Process in a Tidal Flow Constructed Adsorption Effect and Mechanism of Aqueous Arsenic on FeMnNi-LDHs Combined Use of Zirconium-Modified Bentonite Capping and Calcium Nitrate Addition to Control the Release of Phosphorus from Sedin Distribution Characteristics of Antibiotics and Antibiotic Resistance Genes in Wastewater Treatment Plants Occurrence of Antibiotic Resistance Genes and Bacterial Community Structure of Different Sludge Samples During Microwave Pretreatm Selenium Threshold for the Delimitation of Natural Selenium-Enriched Land Improved Regression Kriging Prediction of the Spatial Distribution of the Soil Cadmium by Integrating Natural and Human Factors Simulation Cadmium (Cd) Accumulation in Typical Paddy Soils in South China Bioaccessibility and Health Risks of the Heavy Metals in Soil-Rice System of Southwest Fujian Province Effects of Nano Material on Cadmium Accumulation Capacity and Grain Yield of Indica Hybrid Rice Under Wetting-drying Alternation Regulation Control of a Tribasic Amendment on the Chemical Fractions of Cd and As in Paddy Soil and Their Accumulation in Rice Combined Effect of Weathered Coal Based Amendments and Soil Water Management on Methylmercury Accumulation in Paddy Soil and Effects of Fertilization Strategies on the Cadmium Resistance of Paddy Soil Microorganisms Soil Enzyme Activity in Picea schrenkiana and Its Relationship with Environmental Factors in the Tianshan Mountains, Xinjiang Effects of Biochar on Soil Enzyme Activity & the Bacterial Community and Its Mechanism Effects of Vegetation Restoration on the Structure and Function of the Rhizosphere Soil Bacterial Community of Solanum rostratum Effects of Vegetation Restoration on the Structure and Function of the Rhizosphere Soil Bacterial Community of Solanum rostratum	
Effect of Filter Medium on the Enhancement of Complete Autotrophic Nitrogen Removal over Nitrite Process in a Tidal Flow Constructed Adsorption Effect and Mechanism of Aqueous Arsenic on FeMnNi-LDHs Combined Use of Zirconium-Modified Bentonite Capping and Calcium Nitrate Addition to Control the Release of Phosphorus from Sedin 2 Distribution Characteristics of Antibiotics and Antibiotic Resistance Genes in Wastewater Treatment Plants Occurrence of Antibiotic Resistance Genes and Bacterial Community Structure of Different Sludge Samples During Microwave Pretreatm Selenium Threshold for the Delimitation of Natural Selenium-Enriched Land 5 Improved Regression Kriging Prediction of the Spatial Distribution of the Soil Cadmium by Integrating Natural and Human Factors 5 Simulation Cadmium (Cd) Accumulation in Typical Paddy Soils in South China 6 Bioaccessibility and Health Risks of the Heavy Metals in Soil-Rice System of Southwest Fujian Province 7 Effects of Nano Material on Cadmium Accumulation Capacity and Grain Yield of Indica Hybrid Rice Under Wetting-drying Alternation 7 Regulation Control of a Tribasic Amendment on the Chemical Fractions of Cd and As in Paddy Soil and Their Accumulation in Rice 7 Combined Effect of Weathered Coal Based Amendments and Soil Water Management on Methylmercury Accumulation in Paddy Soil and Effects of Fertilization Strategies on the Cadmium Resistance of Paddy Soil Microorganisms 7 Soil Enzyme Activity in Picea schrenkiana and Its Relationship with Environmental Factors in the Tianshan Mountains, Xinjiang 7 Effects of Fertilization Strategies on the Cadmium Resistance of Paddy Soil Microorganisms 8 Soil Enzyme Activity & the Bacterial Community and Its Mechanism 7 Effects of Vegetation Restoration on the Structure and Function of the Rhizosphere Soil Bacterial Community of Solanum rostratum 7 Response of Microbial Biomass Carbon and Nitrogen and Rice Quality in a Yellow Soil Paddy Field to Biochar Combined with Nitrogen	
Effect of Filter Medium on the Enhancement of Complete Autotrophic Nitrogen Removal over Nitrite Process in a Tidal Flow Constructe Adsorption Effect and Mechanism of Aqueous Arsenic on FeMnNi-LDHs Combined Use of Zirconium-Modified Bentonite Capping and Calcium Nitrate Addition to Control the Release of Phosphorus from Sedin Distribution Characteristics of Antibiotics and Antibiotic Resistance Genes in Wastewater Treatment Plants Occurrence of Antibiotic Resistance Genes and Bacterial Community Structure of Different Sludge Samples During Microwave Pretreatm Selenium Threshold for the Delimitation of Natural Selenium-Enriched Land Improved Regression Kriging Prediction of the Spatial Distribution of the Soil Cadmium by Integrating Natural and Human Factors Simulation Cadmium (Cd) Accumulation in Typical Paddy Soils in South China Bioaccessibility and Health Risks of the Heavy Metals in Soil-Rice System of Southwest Fujian Province Effects of Nano Material on Cadmium Accumulation Capacity and Grain Yield of Indica Hybrid Rice Under Wetting-drying Alternation Regulation Control of a Tribasic Amendment on the Chemical Fractions of Cd and As in Paddy Soil and Their Accumulation in Rice Combined Effect of Weathered Coal Based Amendments and Soil Water Management on Methylmercury Accumulation in Paddy Soil and Effects of Fertilization Strategies on the Cadmium Resistance of Paddy Soil Microorganisms Soil Enzyme Activity in Picea schrenkiana and Its Relationship with Environmental Factors in the Tianshan Mountains, Xinjiang Effects of Farmland Abandonment on Soil Enzymatic Activity and Enzymatic Stoichiometry in the Loess Hilly Region, China Effect of Biochar on Soil Enzyme Activity & the Bacterial Community and Its Mechanism Effects of Vegetation Restoration on the Structure and Function of the Rhizosphere Soil Bacterial Community of Solanum rostratum Response of Microbial Biomass Carbon and Nitrogen and Rice Quality in a Yellow Soil Paddy Field to Biochar Combined with Nitrogen	CHEN You-yuan, LI Pei-qiang, LI Xian-chi, et al. (274) d Wetland
Effect of Filter Medium on the Enhancement of Complete Autotrophic Nitrogen Removal over Nitrite Process in a Tidal Flow Constructe Adsorption Effect and Mechanism of Aqueous Arsenic on FeMnNi-LDHs Combined Use of Zirconium-Modified Bentonite Capping and Calcium Nitrate Addition to Control the Release of Phosphorus from Sedin Distribution Characteristics of Antibiotics and Antibiotic Resistance Genes in Wastewater Treatment Plants Coccurrence of Antibiotic Resistance Genes and Bacterial Community Structure of Different Sludge Samples During Microwave Pretreatm Selenium Threshold for the Delimitation of Natural Selenium-Enriched Land Improved Regression Kriging Prediction of the Spatial Distribution of the Soil Cadmium by Integrating Natural and Human Factors Simulation Cadmium (Cd) Accumulation in Typical Paddy Soils in South China Bioaccessibility and Health Risks of the Heavy Metals in Soil-Ricce System of Southwest Fujian Province Effects of Nano Material on Cadmium Accumulation Capacity and Grain Yield of Indica Hybrid Rice Under Wetting-drying Alternation Regulation Control of a Tribasic Amendment on the Chemical Fractions of Cd and As in Paddy Soil and Their Accumulation in Rice Combined Effect of Weathered Coal Based Amendments and Soil Water Management on Methylmercury Accumulation in Paddy Soil and Effects of Fertilization Strategies on the Cadmium Resistance of Paddy Soil Microorganisms Soil Enzyme Activity in Picea schrenkiana and Its Relationship with Environmental Factors in the Tianshan Mountains, Xinjiang Effects of Fermland Abandonment on Soil Enzymatic Activity and Enzymatic Stoichiometry in the Loess Hilly Region, China Effect of Biochar on Soil Enzyme Activity & the Bacterial Community and Its Mechanism Effects of Vegetation Restoration on the Structure and Function of the Rhizosphere Soil Bacterial Community of Solanum rostratum Response of Microbial Biomass Carbon and Nitrogen and Rice Quality in a Yellow Soil Paddy Field to Biochar Combined with Nitrogen	
Effect of Filter Medium on the Enhancement of Complete Autotrophic Nitrogen Removal over Nitrite Process in a Tidal Flow Constructed Adsorption Effect and Mechanism of Aqueous Arsenic on FeMnNi-LDHs Combined Use of Zirconium-Modified Bentonite Capping and Calcium Nitrate Addition to Control the Release of Phosphorus from Section Control Characteristics of Antibiotics and Antibiotic Resistance Genes in Wastewater Treatment Plants Occurrence of Antibiotic Resistance Genes and Bacterial Community Structure of Different Sludge Samples During Microwave Pretreatm Selenium Threshold for the Delimitation of Natural Selenium-Enriched Land Improved Regression Kriging Prediction of the Spatial Distribution of the Soil Cadmium by Integrating Natural and Human Factors Simulation Cadmium (Cd) Accumulation in Typical Paddy Soils in South China Bioaccessibility and Health Risks of the Heavy Metals in Soil-Rice System of Southwest Fujian Province Effects of Nano Material on Cadmium Accumulation Capacity and Grain Yield of Indica Hybrid Rice Under Wetting-drying Alternation Regulation Control of a Tribasic Amendment on the Chemical Fractions of Cd and As in Paddy Soil and Their Accumulation in Rice Combined Effect of Weathered Coal Based Amendments and Soil Water Management on Methylmercury Accumulation in Paddy Soil and Effects of Fertilization Strategies on the Cadmium Resistance of Paddy Soil Microorganisms Soil Enzyme Activity in Picea schrenkiana and Its Relationship with Environmental Factors in the Tianshan Mountains, Xinjiang Effects of Fermland Abandonment on Soil Enzymatic Activity and Enzymatic Stoichiometry in the Loess Hilly Region, China Effects of Vegetation Restoration on the Structure and Function of the Rhizosphere Soil Bacterial Community of Solanum rostratum Response of Microbial Biomass Carbon and Nitrogen and Rice Quality in a Yellow Soil Paddy Field to Biochar Combined with Nitrogen Effects of Adding Straw and Biochar with Equal Carbon Content on Soil Respiration and Microbial	
Effect of Filter Medium on the Enhancement of Complete Autotrophic Nitrogen Removal over Nitrite Process in a Tidal Flow Constructed Adsorption Effect and Mechanism of Aqueous Arsenic on FeMnNi-LDHs Combined Use of Zirconium-Modified Bentonite Capping and Calcium Nitrate Addition to Control the Release of Phosphorus from Sedin Sedin Construction of Characteristics of Antibiotics and Antibiotic Resistance Genes in Wastewater Treatment Plants Occurrence of Antibiotic Resistance Genes and Bacterial Community Structure of Different Sludge Samples During Microwave Pretreatm Selenium Threshold for the Delimitation of Natural Selenium-Enriched Land Improved Regression Kriging Prediction of the Spatial Distribution of the Soil Cadmium by Integrating Natural and Human Factors Simulation Cadmium (Cd) Accumulation in Typical Paddy Soils in South China Bioaccessibility and Health Risks of the Heavy Metals in Soil-Rice System of Southwest Fujian Province Effects of Nano Material on Cadmium Accumulation Capacity and Grain Yield of Indica Hybrid Rice Under Wetting-drying Alternation Regulation Control of a Tribasic Amendment on the Chemical Fractions of Cd and As in Paddy Soil and Their Accumulation in Rice Combined Effect of Weathered Coal Based Amendments and Soil Water Management on Methylmercury Accumulation in Paddy Soil and Effects of Fertilization Strategies on the Cadmium Resistance of Paddy Soil Microorganisms Soil Enzyme Activity in Picea schrenkiana and Its Relationship with Environmental Factors in the Tianshan Mountains, Xinjiang Effects of Farmland Abandonment on Soil Enzymatic Activity and Enzymatic Stoichiometry in the Loess Hilly Region, China Effects of Vegetation Restoration on the Structure and Function of the Rhizosphere Soil Bacterial Community of Solanum rostratum Effects of Adding Straw and Biochar with Equal Carbon Content on Soil Respiration and Microbial Biomass Carbon and Nitrogen Effects of Adding Straw and Biochar with Equal Carbon Content on Soil Respiration and Microbial Biomass	
Effect of Filter Medium on the Enhancement of Complete Autotrophic Nitrogen Removal over Nitrite Process in a Tidal Flow Constructed Adsorption Effect and Mechanism of Aqueous Arsenic on FeMnNi-LDHs Combined Use of Zirconium-Modified Bentonite Capping and Calcium Nitrate Addition to Control the Release of Phosphorus from Section Control Characteristics of Antibiotics and Antibiotic Resistance Genes in Wastewater Treatment Plants Occurrence of Antibiotic Resistance Genes and Bacterial Community Structure of Different Sludge Samples During Microwave Pretreatm Selenium Threshold for the Delimitation of Natural Selenium-Enriched Land Improved Regression Kriging Prediction of the Spatial Distribution of the Soil Cadmium by Integrating Natural and Human Factors Simulation Cadmium (Cd) Accumulation in Typical Paddy Soils in South China Bioaccessibility and Health Risks of the Heavy Metals in Soil-Rice System of Southwest Fujian Province Effects of Nano Material on Cadmium Accumulation Capacity and Grain Yield of Indica Hybrid Rice Under Wetting-drying Alternation Regulation Control of a Tribasic Amendment on the Chemical Fractions of Cd and As in Paddy Soil and Their Accumulation in Rice Combined Effect of Weathered Coal Based Amendments and Soil Water Management on Methylmercury Accumulation in Paddy Soil and Effects of Fertilization Strategies on the Cadmium Resistance of Paddy Soil Microorganisms Soil Enzyme Activity in Picea schrenkiana and Its Relationship with Environmental Factors in the Tianshan Mountains, Xinjiang Effects of Fermland Abandonment on Soil Enzymatic Activity and Enzymatic Stoichiometry in the Loess Hilly Region, China Effects of Vegetation Restoration on the Structure and Function of the Rhizosphere Soil Bacterial Community of Solanum rostratum Response of Microbial Biomass Carbon and Nitrogen and Rice Quality in a Yellow Soil Paddy Field to Biochar Combined with Nitrogen Effects of Adding Straw and Biochar with Equal Carbon Content on Soil Respiration and Microbial	
Effect of Filter Medium on the Enhancement of Complete Autotrophic Nitrogen Removal over Nitrite Process in a Tidal Flow Constructed Adsorption Effect and Mechanism of Aqueous Arsenic on FeMnNi-LDHs Combined Use of Zirconium-Modified Bentonite Capping and Calcium Nitrate Addition to Control the Release of Phosphorus from Sedin Sedin Construction of Characteristics of Antibiotics and Antibiotic Resistance Genes in Wastewater Treatment Plants Occurrence of Antibiotic Resistance Genes and Bacterial Community Structure of Different Sludge Samples During Microwave Pretreatm Selenium Threshold for the Delimitation of Natural Selenium-Enriched Land Improved Regression Kriging Prediction of the Spatial Distribution of the Soil Cadmium by Integrating Natural and Human Factors Simulation Cadmium (Cd) Accumulation in Typical Paddy Soils in South China Bioaccessibility and Health Risks of the Heavy Metals in Soil-Rice System of Southwest Fujian Province Effects of Nano Material on Cadmium Accumulation Capacity and Grain Yield of Indica Hybrid Rice Under Wetting-drying Alternation Regulation Control of a Tribasic Amendment on the Chemical Fractions of Cd and As in Paddy Soil and Their Accumulation in Rice Combined Effect of Weathered Coal Based Amendments and Soil Water Management on Methylmercury Accumulation in Paddy Soil and Effects of Fertilization Strategies on the Cadmium Resistance of Paddy Soil Microorganisms Soil Enzyme Activity in Picea schrenkiana and Its Relationship with Environmental Factors in the Tianshan Mountains, Xinjiang Effects of Farmland Abandonment on Soil Enzymatic Activity and Enzymatic Stoichiometry in the Loess Hilly Region, China Effects of Vegetation Restoration on the Structure and Function of the Rhizosphere Soil Bacterial Community of Solanum rostratum Effects of Adding Straw and Biochar with Equal Carbon Content on Soil Respiration and Microbial Biomass Carbon and Nitrogen Effects of Adding Straw and Biochar with Equal Carbon Content on Soil Respiration and Microbial Biomass	
Effect of Filter Medium on the Enhancement of Complete Autotrophic Nitrogen Removal over Nitrite Process in a Tidal Flow Constructed Adsorption Effect and Mechanism of Aqueous Arsenic on FeMnNi-LDHs Combined Use of Zirconium-Modified Bentonite Capping and Calcium Nitrate Addition to Control the Release of Phosphorus from Sedin Distribution Characteristics of Antibiotics and Antibiotic Resistance Genes in Wastewater Treatment Plants Occurrence of Antibiotic Resistance Genes and Bacterial Community Structure of Different Sludge Samples During Microwave Pretreatment Plants Selenium Threshold for the Delimitation of Natural Selenium-Enriched Land Improved Regression Kriging Prediction of the Spatial Distribution of the Soil Cadmium by Integrating Natural and Human Factors Simulation Cadmium (Cd) Accumulation in Typical Paddy Soils in South China Bioaccessibility and Health Risks of the Heavy Metals in Soil-Rice System of Southwest Fujian Province Effects of Nano Material on Cadmium Accumulation Capacity and Grain Yield of Indica Hybrid Rice Under Wetting-drying Alternation Regulation Control of a Tribasic Amendment on the Chemical Fractions of Cd and As in Paddy Soil and Their Accumulation in Rice Combined Effect of Weathered Coal Based Amendments and Soil Water Management on Methylmercury Accumulation in Paddy Soil and Effects of Farmland Abandonment on Soil Enzymatic Activity and Enzymatic Stoichiometry in the Loess Hilly Region, China Effects of Farmland Abandonment on Soil Enzymatic Activity and Enzymatic Stoichiometry in the Loess Hilly Region, China Effects of Vegetation Restoration on the Structure and Function of the Rhizosphere Soil Bacterial Community of Solanum rostratum Effects of Adding Straw and Biochar with Equal Carbon Content on Soil Respiration and Microbial Biomass Carbon and Nitrogen and Rice Quality in a Yellow Soil Paddy Field to Biochar Combined with Nitrogen Effects of Adding Straw and Biochar with Equal Carbon Content on Soil Respiration and Microbial Biomass Carbon and Nitroge	CHEN You-yuan, LI Pei-qiang, LI Xian-chi, et al. (274) d Wetland
Effect of Filter Medium on the Enhancement of Complete Autotrophic Nitrogen Removal over Nitrite Process in a Tidal Flow Constructed Adsorption Effect and Mechanism of Aqueous Arsenic on FeMnNi-LDHs Combined Use of Zirconium-Modified Bentonite Capping and Calcium Nitrate Addition to Control the Release of Phosphorus from Sedin Distribution Characteristics of Antibiotics and Antibiotic Resistance Genes in Wastewater Treatment Plants Occurrence of Antibiotic Resistance Genes and Bacterial Community Structure of Different Studge Samples During Microwave Pretreatm Selenium Threshold for the Delimitation of Natural Selenium-Enriched Land Note Improved Regression Kriging Prediction of the Spatial Distribution of the Soil Cadmium by Integrating Natural and Human Factors Simulation Cadmium (Cd) Accumulation in Typical Paddy Soils in South China Bioaccessibility and Health Risks of the Heavy Metals in Soil-Rice System of Southwest Fujian Province Effects of Nano Material on Cadmium Accumulation Capacity and Grain Yield of Indica Hybrid Rice Under Wetting-drying Alternation Regulation Control of a Tribasic Amendment on the Chemical Fractions of Cd and As in Paddy Soil and Their Accumulation in Rice Combined Effect of Weathered Coal Based Amendments and Soil Water Management on Methylmercury Accumulation in Paddy Soil and Effects of Fertilization Strategies on the Cadmium Resistance of Paddy Soil Microorganisms Soil Enzyme Activity in Picea schrenkiana and Its Relationship with Environmental Factors in the Tianshan Mountains, Xinjiang Effects of Farmland Abandonment on Soil Enzymeatic Activity and Enzymatic Stoichiometry in the Loess Hilly Region, China Effects of Vegetation Restoration on the Structure and Function of the Rhizosphere Soil Bacterial Community of Solanum rostratum Response of Microbial Biomass Carbon and Nitrogen and Rice Quality in a Yellow Soil Paddy Field to Biochar Combined with Nitrogen How Different Ratios of Straw Incorporation to Nitrogen Fertilization Influence Endogenous	
Effect of Filter Medium on the Enhancement of Complete Autotrophic Nitrogen Removal over Nitrite Process in a Tidal Flow Constructed Adsorption Effect and Mechanism of Aqueous Arsenic on FeMnNi-LDHs Combined Use of Zirconium-Modified Bentonite Capping and Calcium Nitrate Addition to Control the Release of Phosphorus from Sedin Distribution Characteristics of Antibiotics and Antibiotic Resistance Genes in Wastewater Treatment Plants Occurrence of Antibiotic Resistance Genes and Bacterial Community Structure of Different Sludge Samples During Microwave Pretreatment Plants Selenium Threshold for the Delimitation of Natural Selenium-Enriched Land Improved Regression Kriging Prediction of the Spatial Distribution of the Soil Cadmium by Integrating Natural and Human Factors Simulation Cadmium (Cd) Accumulation in Typical Paddy Soils in South China Bioaccessibility and Health Risks of the Heavy Metals in Soil-Rice System of Southwest Fujian Province Effects of Nano Material on Cadmium Accumulation Capacity and Grain Yield of Indica Hybrid Rice Under Wetting-drying Alternation Regulation Control of a Tribasic Amendment on the Chemical Fractions of Cd and As in Paddy Soil and Their Accumulation in Rice Combined Effect of Weathered Coal Based Amendments and Soil Water Management on Methylmercury Accumulation in Paddy Soil and Effects of Farmland Abandonment on Soil Enzymatic Activity and Enzymatic Stoichiometry in the Loess Hilly Region, China Effects of Farmland Abandonment on Soil Enzymatic Activity and Enzymatic Stoichiometry in the Loess Hilly Region, China Effects of Vegetation Restoration on the Structure and Function of the Rhizosphere Soil Bacterial Community of Solanum rostratum Effects of Adding Straw and Biochar with Equal Carbon Content on Soil Respiration and Microbial Biomass Carbon and Nitrogen and Rice Quality in a Yellow Soil Paddy Field to Biochar Combined with Nitrogen Effects of Adding Straw and Biochar with Equal Carbon Content on Soil Respiration and Microbial Biomass Carbon and Nitroge	CHEN You-yuan, LI Pei-qiang, LI Xian-chi, et al. (274) d Wetland